

Hochschule für Angewandte Wissenschaften Hamburg

Hamburg University of Applied Sciences

Bachelor Thesis

Jonas Nierendorf

Entwicklung eines Konzepts zur Temperierung eines Prüfstands für oszillierende Wälzlager

Fakultät Technik und Informatik Studiendepartment Maschinenbau und Produktion Faculty of Engineering and Computer Science Department of Mechanical Engineering and Production

Jonas Nierendorf

Entwicklung eines Konzepts zur Temperierung eines Prüfstands für oszillierende Wälzlager

Bachelor Thesis eingereicht im Rahmen der Bachelorprüfung

im Studiengang Bachelor of Science Maschinenbau und Produktion, Energie- und Anlagensysteme

am Department Maschinenbau und Produktion der Fakultät Technik und Informatik der Hochschule für Angewandte Wissenschaften Hamburg

Betreuender Prüfer: Prof. Peter Dalhoff Zweitgutachter: Dr. Matthias Stammler

Eingereicht am: 25.09.2024

Jonas Nierendorf

Thema der Arbeit

Entwicklung eines Konzepts zur Temperierung eines Prüfstands für oszillierende Wälzlager

Stichworte

Windenergie, Pitchlager, Wälzlagerprüfstände, Temperiersysteme, Wärmeleitung, thermische Modellierung

Kurzzusammenfassung

In dieser Bachelorarbeit wurde ein konzeptioneller Entwurf für ein Temperiersystem für einen Wälzlagerprüfstand erarbeitet. Als Zieltemperatur wurde -30°C am Außenring des Lagers festgelegt. Um einen Einstieg in das Thema Tieftemperaturen zu gewährleisten wurden moderne Kühlmethoden, Dämmstoffe und Wärmeleiter vorgestellt. Anhand einer Testkampagne mit einem geliehenem Kühlaggregat wurde das Betriebsverhalten der Komponenten des Prüfstandes bei Temperaturen unter 0°C beobachtet, sowie die zusätzlichen Arbeitsschritte beim Lagertausch analysiert. Mit den gewonnen Erkenntnissen wurde aus einer Auswahl von 9 Temperiersystemen ein geeignetes Temperiersystem empfohlen. Für dieses System wurde ein passendes Dämmungskonzept entwickelt. Abschließend wurde ein thermisches Modell in Simulink erstellt und mit experimentellen Daten validiert.

Title of the paper

Developing of a concept for a temperature system for a test rig for oscillating rolling element bearings

Keywords

wind energy, pitch bearings, test rigs for bearings, temperature systems, heat transfer, thermal modelling

Abstract

In this bachelor's thesis, a conceptual design of a temperature system for a bearing test rig was created, to allow test runs at a bearing temperature of -30°C. Therefore, state of the art cooling methods, and insulation and heat conducting materials were introduced. With a rented cooling unit, the behaviour of the test rig at temperatures below 0°C was observed, and the influence on the bearing exchange workflow was analyzed. With the gathered knowledge, a recommendation for a system was made from a collection of temperature systems. For this system, an insulation was designed. Finally a thermal model was created and validated with experimental data.

Contents

1	Intr	oduction	1
	1.1	Oscillating rolling element bearings in wind turbines	1
	1.2	Greases in pitch bearings	3
	1.3	Temperature conditions of wind turbines	3
	1.4	Scope of this thesis	4
2	Fun	damentals	5
	2.1	Thermodynamic	5
	2.2	Heat transfer	7
	2.3	MATLAB and Simulink	9
3	Stat	te of the art	11
	3.1	Cooling methods	11
		3.1.1 Vapor compression cycle	11
		3.1.2 Cold by phase change	15
		3.1.3 Thermo electric effect	16
	3.2	Materials	18
		3.2.1 Thermal conductive materials	18
		3.2.2 Thermal insulation materials	18
	3.3	Existing test rigs with temperature systems	19
		3.3.1 Test rig of Mannheim Tribology Competence Center (KTM)	19
		3.3.2 Test rig of Institute of Machine Design and Tribology (IMKT) at Leibniz	
		University of Hanover	21
	3.4	IWES test rig BEAT0.2	21
		3.4.1 Scaling of real wind turbine pitch conditions for pitch bearings	22
		3.4.2 Layout of the test rig	23
		3.4.3 Analysis of results	24
4	Low	v temperature tests with a rented cooling unit	25
	4.1	Changes of layout and insulation	25
	4.2	Bearing exchange work flow	27
	4.3	Test results	29
	4.4	Acquired knowledge	29
5	Eva	luation of temperature systems	31
	5 1	Climate Chambers	32

Contents

9	Out	look	67
8	Con	clusion	65
		7.5.2 Comparison between simulated and experimental data	62
		7.5.1 Validation process	61
	7.5	Validation	61
	7.4	Connection of test rig and cooling unit	55
	7.3	Modelling of the bearing	54
	7.2	Geometrical and thermal simplification of the test rig	50
	7.1	Basic structure of the model	49
7	The	rmal model	49
	6.3	Conclusion of the chosen characteristics	48
	6.2	Manifestations of the parameters	45
	6.1	Insulation specifications	45
6	Insu	lation design	45
	5.5	Final rating	43
	5.4	Considerations which apply to all concepts	43
	5.3	Peltier elements	42
		5.2.6 Thermal fluid bath	41
		5.2.5 Cooling coil around the housing	40
		5.2.4 Axial cooling holes inside the housing	39
		5.2.3 Heat sink between the bearings	38
		5.2.2 Cooling tube in a groove on the outside of the housing	37
		5.2.1 Cooling ducts inside the bearing seat	35
	5.2	Cooling unit solutions	35

List of Tables

3.1	Collection of thermal conducting materials	18
3.2	Collection of thermal insulating materials	19
4.1	Specification of the rented cooling unit	25
4.2	Cooling capacity of the cooling unit	25
4.3	Changed work steps for low temperature tests	29
5.1	Conversion and weight of the criteria	43
5.2	Scoring of the rating	44
5.3	Rating of the temperature systems	44
6.1	Morphological box for the choice of insulation	45
6.2	Morphological box for the choice of isolation	47
7.1	Material Properties	52
7.2	Experimental data for validation	62
7.3	Experimental and simulated data	62

List of Figures

1.1	Layout of a ball bearing [62]	1
1.2	Pitch movement around z-axis [41]	2
1.3	Cycle comparison of CPC and IPC Systems [57]	2
1.4	Bearing temperature vs. life for mineral oil greases [4]	4
2.1	Principle of the vapor compression cycle [33]	7
3.1	Working principle of a cooling unit [51]	12
3.2	Cooling capacity loss of cooling units from manufacturer Huber [50]	13
3.3	Air flow inside a climate chamber [58]	14
3.4	Cross sectional view of climate chamber from the TU Ilmenau [26]	15
3.5	Working principle of Peltier (left) and Seebeck (right) effect [63]	16
3.6	Common Peltier element (left, middle) [35] and a multi-stage Peltier element	
	(right) [61]	17
3.7	Peltier cooling element for climate chambers [24]	17
3.8	Flexible synthetic rubber (left), insulation bag (middle), and vacuum insulated	
	panels (right)	19
3.9	Oscillating Rolling Wear Test Bench of KTM [31]	20
3.10	Cylindrical cover to insulate the bearing [31]	20
3.11	Test rig of the IMKT [17]	21
3.12	Visualization of x/2b ratio [55]	22
3.13	Four-point contact ball bearing (left)[20] and two angular contact ball bearings	
	in x-configuration (right) [13]	22
3.14	x/2b amplitude ratios of IWES IWT-7.5-164 Reference Turbine [2]	23
3.15	Layout of BEAT0.2 test rig [2]	23
3.16	Shaft without bearings next to drive, torque meter and housing	24
4.1	Copper coil wrapped around the housing	26
4.2	Ice around coupling and shaft	27
4.3	Insulation of the valves	27
4.4	Insulated test rig	28
5.1	Schematic of smallest cuboid	33
5.2	cooling ducts in serial (left) and parallel (right)	36
5.3	Cooling ducts inside the bearing seat	36
6.1	Concentional design of the insulation, without cooling hoses	48

List of Figures

7.1	calculation of the temperature (left) and the final subsystem (right)	49
7.2	Calculation of a heat flow (left) and the final subsystem (right)	50
7.3	Section view and front view of a CAD Model of BEAT0.2 and its chosen sim-	
	plifications. This view, the front view, and the back view are also on the CD	
	enclosed with this document	51
7.4	Heat flows of c3	53
7.5	Simulink subsystem of component c3	54
7.6	Simplification of the bearing at first bearing position	55
7.7	Cooling capacity of the cooling unit	56
7.8	The cooling unit as a subsystem	57
7.9	Hose subsystem in Simulink	58
7.10	Discretization of the gap between cooling coil and housing	59
7.11	Cooling coil as a subsystem in Simulink	60
7.12	Thermal model in Simulink	60
7.13	Temperature program for validation	61

List of symbols

Symbol	Unit	Description
$-$ * $_r$, r	m	Inner radius
$*_R, R$	m	Outer radius
$*_x$	m	X-dimension of a component
$*_y$	m	Y-dimension of a component
$*_Z$	m	Z-dimension of a component
A	m^2	Area
c_p	$\frac{J}{kgK}$	Specific heat capacity
Δ	-	Change of the variable
EER	-	Energy efficiency ratio
ϵ	_	Emissivity
η_c	-	Carnot efficiency
G	$\frac{\frac{W}{K}}{\frac{W}{K}}$	Thermal conductance
k	$\frac{W}{m K}$	Thermal conductivity
l	m	Length
ln	-	Natural logarithm
m	kg	Mass
\dot{m}	$\frac{kg}{s}$	Mass flow
n_{pump}	$\frac{s_1}{min}$	Pump speed rate
n_{re}	-	Number of rolling elements
$ abla^2$	_	Spatial derivative of a variable
P	W	Power
Q	J	Heat energy
\dot{Q}	W	Heat flow
r_m	m	Radius inside a ring, where the outer part and inner part have the same area
ho	$\frac{kg}{m^3}$	Density
s	m	Thickness
σ	$\frac{W}{m^2 K^4}$	Stefan Boltzmann-Constant
T	$K, {}^{\circ}C$	Temperature
T_c	K	Temperature of the cold system
T_h	K	Temperature of the hot system
\dot{V}	$\frac{m^3}{2}$	Volume flow rate
W	$\overset{s}{J}$	Work
U	J	Internal energy

List of abbreviations

Abbreviation	Description				
BEAT	Bearing endurance and acceptance test rig				
CAD	Computer aided design				
CPC	Collective pitch control				
EPS	Expanded Polystyrol				
IPC	Individual pitch control				
IWES	Institute for Wind Energy Systems				
MDF	Medium-density fibreboard				
OSB	oriented strand board				
PU	Polyurethane				
RMSE	Root mean square error				
TIM	Thermal interface Materials				
XPS	Extruded Polystyrol				

1 Introduction

1.1 Oscillating rolling element bearings in wind turbines

Bearings are commonly used to reduce wear between two parts with a relative motion to each other. There are journal bearings and rolling element bearings. In case of the relative motion being a rotation about on axis, rolling element bearings consist of an outer ring, an inner ring, rolling elements like balls or rollers, a cage or separators which hold the rolling elements in place (Figure 1.1) and a lubricant between the components. If the outer or the inner ring rotates around the other, the rolling elements will perform a rolling movement between those two components. This results in an almost sliding free motion with low friction. In a typical application of rolling element bearings, henceforth referred to as bearings, the inner or outer ring revolves millions of rotations in the same direction. In some applications like in pitch bearings of wind turbines the bearings perform oscillating movements of just a few degrees.

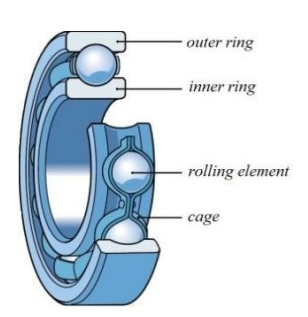


Figure 1.1: Layout of a ball bearing [62]

The nacelle is on the top of the tower of a wind turbine. The hub is connected to the nacelle by the main bearing. The rotor blades are connected to the hub by pitch bearings. A pitch bearing allows the rotor blade to rotate on its own z-axis, shown in Figure 1.2. This movement changes the angle of attack of the airflow and with that the amount of lift on the blade. The load of the turbine and the produced power depend on lift. If the lift is reduced, the load and the produced power also decrease. This is useful at very high wind speed to prevent an overload of the turbine or to achieve a constant power output above rated wind speed. If the pitch control

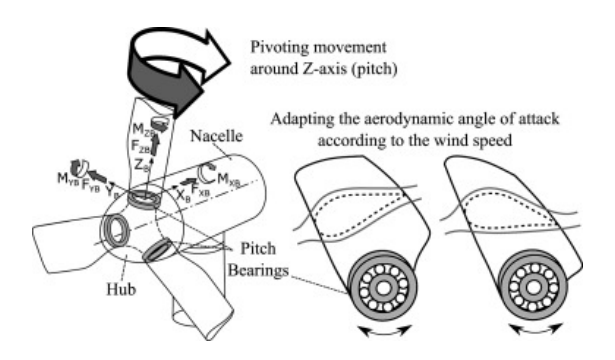


Figure 1.2: Pitch movement around z-axis [41]

systems pitch all blades the same amount by the same time it is called collective pitch control system (CPC). Some turbine models support an individual pitch control system (IPC). Each blade can change its pitch angle and therefor the angle of attack individually. Wind speed differences over the rotor diameter and the flow decelerating effect of the tower cause load differences within a full rotor rotation. The technology of an individual pitch system is used to compensate those load differences.

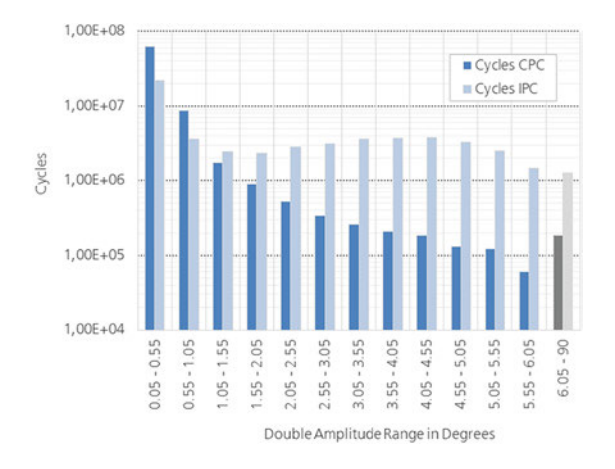


Figure 1.3: Cycle comparison of CPC and IPC Systems [57]

The pitch cycle comparison of CPC and IPC system of the IWES IWT-7.5-164 Reference Turbine is shown in Figure 1.3. A double amplitude is the distance of a rotational movement to a turning point and back to the next turning point. The figure clarifies, that the highest cycle share is done with very small double amplitudes. Under constant movement and load, rolling element bearings are supposed to form a small film of lubricant between raceway and rolling elements. Those small double amplitudes shown in Figure 1.3 do not allow constant, but high frequent movement and that prevent the formation of such a lubricant film. Additionally the high

contact pressure in pitch bearings squeezes the lubricant out of the contact zone [42], and wear on rolling elements and raceways can occur [14].

1.2 Greases in pitch bearings

Lubricants are also used to reduce wear and friction between two parts with a relative motion to each other. There are 4 different types of lubricants: Solid (i.e. graphite), liquid (i.e. synthetic oil), gaseous (i.e. air), and semi-solid (greases) [25]. Since the high loads in pitch bearings eliminate solid lubricants, the high energy demand for air lubrication and high deformations which make a tight liquid lubrication very cost-intensive, greases are the common choice of lubricants in pitch bearings.

Greases consist of a thickener, oil, and additives. The thickener provides oil at shear stress, and absorbs and stores it when there is no shear stress. Shear stress is caused by relative movements between rolling elements and raceways. The behavior of providing and absorbing oil is called bleeding rate. Together with the base oil viscosity they form the main characteristics of greases. In Schwack 2020 [41] six different greases were investigated for small oscillations. Test results showed that greases with low viscosity and high bleeding rate had the best performance.

Spikes 1990 [54] proved in his work, that viscosity has a high dependency on temperature and pressure. Porfiryev 2020 [37] showed, that the temperature has an effect on thickening capacity and colloidal stability of the thickener. In Booser 2010 [4] the effect of temperature on grease life in rotating ball bearings was investigated and the results showed a significant reduction of life time outside the common industrial temperature range in Figure 1.4.

1.3 Temperature conditions of wind turbines

Typically wind turbines are designed for a temperature range of -10 $^{\circ}$ C to +40 $^{\circ}$ C. The extreme temperature range for standard wind turbines expands to -20 $^{\circ}$ C to +50 $^{\circ}$ C [15]. Since the expansion of wind farms increases, the demand on accessible area will also increase. Areas may be used which have inconvenient temperature conditions and fall below standard temperature range. To realize decentralized energy production concepts, it is also necessary to design wind turbines for cold climate conditions. The IEC 61400-1:2019 guideline [15] defines the following temperature criteria for the wind turbine cold climate class: the ambient temperature for wind

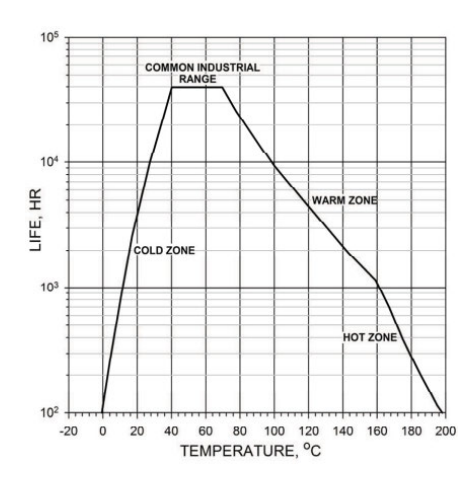


Figure 1.4: Bearing temperature vs. life for mineral oil greases [4]

turbine operation is -30 °C, the expected minimum ambient temperature in hourly average during 1 year is -40°C, the yearly mean ambient temperature is -5°C.

1.4 Scope of this thesis

The Bearing Endurance and Acceptance Test rig BEAT0.2 at the Large Bearing Laboratory of Fraunhofer Institute for Wind Energy Systems is used to run down scaled blade bearing tests for wind turbines. The greases are evaluated on their wear behavior on oscillating angular contact bearings. The tests are currently executed at room temperature but shall be executed at lowest operation temperature for cold climate wind turbines according to IEC 61400-1:2019 [15]. Therefore, a concept shall be developed to achieve down to -30 °C at the bearing. Ideally it is also possible to heat the temperature up to +80°C with the chosen concept. This includes comparing available cooling technologies and the design of an insulation box. Finally, a thermal model of the test rig shall be developed to determine the necessary specifications for the cooling unit.

2 Fundamentals

2.1 Thermodynamic

Thermodynamic systems

A thermodynamic system is a spatial delimited model, whose physical properties can be described by the laws of thermodynamics. The internal energy U of a system includes heat Q and internal work W and is defined by Equation 2.1 [29].

$$U = Q + W (2.1)$$

If energy is supplied to a system, the internal energy of this system increases. This is formulated by the change of internal energy ΔU (Equation 2.2) [29].

$$\Delta U = \Delta Q + \Delta W \tag{2.2}$$

The change in internal energy always results in a change in temperature, which is defined by Equation 2.3 [28].

$$\Delta U = c_p \cdot m \cdot \Delta T \tag{2.3}$$

 c_p is the specific heat capacity and its unit is $[\frac{J}{kg\,K}]$. This material property defines how much energy is necessary to increase the temperature of a system with the mass m. If it is assumed, that no work is performed, ΔU in Equation 2.3 can be replaced by the heat Q and the equation can be rearranged to the change in heat ΔT (Equation 2.4). In addition, the indices t0 and t1 are introduced, to specify the time points.

$$\Delta T_{t0,t1} = \frac{\Delta Q_{t0,t1}}{m \cdot c_p} \tag{2.4}$$

When the change in temperature from moment t0 to moment t1 is calculated with the change in heat from moment t0 to t1, the current temperature T_{t1} can be calculated by adding the initial temperature T_{t0} to the right side of Equation 2.4, which is done in Equation 2.5.

$$T_{t1} = \frac{\Delta Q_{t0,t1}}{m \cdot c_p} + T_{t0} \tag{2.5}$$

 Δ Q can be defined as the integral of the balance of heat flows \dot{Q} , which flow over the system borders. This addition leads to Equation 2.6.

$$T_{t1} = \frac{\int_{t0}^{t1} \sum \dot{Q}(t)}{m \cdot c_p} + T_{t0}$$
 (2.6)

Vapor compression cycle

The second law of thermodynamics says that heat always transfers from higher temperature to lower temperature, if no work is performed. This is the reason why temperatures within a system equalize over time without external influence. Equalizing temperatures are unsuitable for cooling methods, but with externally performed work the direction of heat transfer can be adjusted. Work can be for example the change of pressure. Compression causes a positive change of work and therefore a temperature rise, expansion causes a temperature decrease. An additional factor is the energy demand during the phase change of a substance. When a substance changes its phase from gaseous to liquid, or from liquid to solid, it emits heat. A phase change in the other direction, from solid to liquid and from liquid to gaseous, requires energy. The heat of gaseous to liquid is called heat of condensation and the heat of liquid to gaseous is called heat of evaporation. Both heat therms have the same value, but a different direction. The same applies to condensation temperature and evaporation temperature. The temperature depends on pressure. Higher pressure causes a rise of the temperature, and lower pressure decreases the temperature. This phenomena is utilized in the so called vapor compression cycle. Figure 2.1 is used to describe the vapor compression cycle. It includes three systems: the to be cooled system (A) on the left, the circulating substance (B) in the middle, and the warm environment (C) on the right. [10] The temperature of A is lower than the temperature of C, which disallows a natural heat flow from A to C. To start a cooling process anyway the compressor forces the substance in system B to circulate. The expansion valve generates a higher pressure in the right part of the circulation and a lower pressure in the left part. The low pressure causes the condensation temperature to decrease, ideally below the temperature of system A. The substance condensates and absorbs heat from system A. The

Compressor cool low-pressure gas hot high-pressure gas Evaporator Coil Condenser heat input heat output

Expansion Valve

cold low-pressure liquid

The Vapor-Compression Refrigeration Cycle

Figure 2.1: Principle of the vapor compression cycle [33]

high pressure on the right side causes a temperature rise, the substance vaporizes and releases heat to C. Performed work by the compressor allows a heat transfer from a colder to a warmer system. Usually the theoretical efficiency of a thermodynamic process is calculated with the carnot efficiency η_c (Equation 2.7), where T_c is the temperature of the cold system and T_h is the temperature of the hot system. But in cooling applications the energy efficiency ratio EER (Equation 2.8) is used, where \dot{Q} is the extracted heat flow, respectively the cooling capacity, and P is the supplied power of the compressor. [10]

$$\eta_c = 1 - \frac{T_c}{T_h} \tag{2.7}$$

$$EER = \frac{\dot{Q}}{P} = \frac{T_c}{T_h - T_c} \tag{2.8}$$

warm high-pressure liquid

2.2 Heat transfer

The heat transfer theory describes the exchange in heat energy over thermodynamic system borders. The exchange happens mostly in three ways: heat conduction, heat convection and heat radiation. How much heat is transferred is usually indicated by the heat flow \dot{Q} . It describes how much heat energy Q is transferred within a moment and has the unit $\left[\frac{W}{s}\right]$. [39]

Heat conduction

Heat conduction describes the heat exchange inside a material due to molecular oscillations. When a region of a material is heated, the energy level of the particles rise. The higher the energy level, the higher the oscillating movements of the particles. While oscillating, it comes to collisions with other particles. Due to momentum conservation, the high oscillating particle on higher energy level transfers some energy to the collision particle with lower energy level. How fast a material conducts heat is quantified by the thermal conductivity k. It is a material property and has the unit $\left[\frac{W}{mK}\right]$. The heat flow inside a conducting material depends on the temperature field which can be calculated by Fourier's law (Equation 2.9, here shown without source term), where $\nabla^2 T$ is the second spatial derivative of the temperature T. [39]

$$\rho \cdot c_p \cdot \frac{dT}{dt} = k \cdot \nabla^2 T \tag{2.9}$$

This partial differential equation is unsuitable for practical use, but assumptions (constant k, one-dimensional, stationary) lead to two equations, that simplify the calculation of the heat flow through a wall (Equation 2.10) and through a tube (Equation 2.11). [39] [53]

$$\dot{Q}_{AB,wall} = \frac{A_{AB}}{\sum \frac{k_i}{s_i}} \cdot \Delta T_{AB} \tag{2.10}$$

$$\dot{Q}_{AB,tube} = \frac{2 \cdot \pi \cdot l_{AB}}{\sum \frac{1}{k_i} \cdot ln(\frac{R_i}{r_i})} \cdot \Delta T_{AB}$$
 (2.11)

 A_{AB} is the area of the wall between system A and B. k_i and s_i are the thermal conductivity and the thickness of the individual wall layers. l_{AB} is the length of the tube, and R_i and r_i are the radii of the tube layers. In both cases, the heat flow depends proportionally on the temperature difference. The factors before the temperature difference can be summarized to the conductance G, which gives a general equation for a heat flow by heat conduction (Equation 2.12). For the other direction (from B to A) the algebraic sign is inverted (Equation 2.13).

$$\dot{Q}_{AB} = G_{AB} \cdot \Delta T_{AB} \tag{2.12}$$

$$\dot{Q}_{BA} = -\dot{Q}_{AB} \tag{2.13}$$

Heat convection

Heat convection describes the heat exchange by mass transport, which happens in fluids or gasses. This mass transport can be forced, for example by a fan, which creates an air flow, or

by a pump, which creates a fluid flow. This is called forced convection [39]. But convection can also happen on natural ways, by lift and down flow due to heat induced density differences inside a medium [39]. This is called natural convection or free convection. Heat transfer by forced convection is usually higher than by free convection [39]. The effect of convection on heat transfer is described by the convective heat transfer coefficient h [53]. The flow velocity of a medium is reduced near by a surface, due to friction. Right at the surface the velocity is zero. This velocity gradient takes place in the boundary layer. Because of the reduced velocity the share of convective heat transfer is reduced and heat conduction is increased. This complicates the calculation of h, as multiple partial differential equations have to be solved. In practical applications, h is approximately calculated by dimensionless quantities, like the Reynolds number Re, the Prandtl number Pr, and the Nusselt number Nu. These numbers depend on flow characteristics and material properties of the flowing. The effect of convection over a small layer of gas or fluid between two bodies can be neglected, because the share of heat conduction dominates. [39]

Heat radiation

In case of heat radiation, heat is transferred from one body to another body by electromagnetic waves. The space between the systems must be permeable to these kind of waves. It works best in vacuum, but also gasses allow radiation. The wavelength of the electromagnetic waves is between 0.8 and 400 μm . The intensity of heat radiation of a system increases with increasing surface temperature, but also depends on the emissivity. The receiving of heat radiation depends on the absorbency of the surface. The residual of the heat radiation is reflected or transmitted. Heat radiation is calculated with Equation 2.14. The Boltzmann-Constant σ is $5.67 \cdot 10^{-8} \frac{W}{m^2 K^4}$, A is the surface area of the body, ϵ the emissivity, and T the temperature of the body. The emissivity depends on material and surface properties. [39]

$$\dot{Q}_{radiation} = \epsilon \cdot A \cdot \sigma \cdot T^4 \tag{2.14}$$

The exponent of the temperature shows, that heat radiation has its highest effect at high temperatures.

2.3 MATLAB and Simulink

MATLAB [16] is a coding environment for numerical computation of mathematical problems. It is especially designed for matrix operations, but it is also often used for data analysis

and visualization. It allows the definition of variables, which can be stored in the so called workspace. The function range can be extended by various extensions, so called toolboxes, which fulfil specific tasks. One toolbox is integrated in MATLAB by default, which is Simulink. Simulink is a graphical coding environment which allows the modelling of mathematically describable problems. The model is created by linking different blocks together. These blocks can be mathematical operations like add or subtract, continuous functions like integration or derivation, but also coded MATLAB functions and much more. Every block processes its input signals and produces an output signal. Multiple block links can be summarized as a new block which is called subsystem. Variables of the MATLAB workspace can be loaded into Simulink and be connected to the blocks as input signals. The output signals can be graphically investigated or exported to the MATLAB workspace for further analyzing. Final block combinations can have the form of differential equations. They can be solved by various numerical fixed-step or variable-step approximation solvers. The step size describes the time duration between two Simulation steps. The step size must be small enough, so that the equations give a finite result. But the smaller the step size the more simulation steps are necessary. This increases the execution time. When variable step size is activated, the solver adapts the step size to the dynamic of the simulation. Fixed step size sets the time duration on a constant value. The value can be set manually or calculated by the solver.

3 State of the art

3.1 Cooling methods

In contrast to heat, cold is not a byproduct of energy conversion processes. Therefore, it is a greater challenge to cool down a system instead of heating it up. In the following a collection of cooling methods will be explained in detail.

3.1.1 Vapor compression cycle

The vapor compression cycle is used in cooling units or climate chambers.

Cooing units

In cooling units the vapor compression cycle is included in a 2-stage cooling process. The vapor compression cycle is used to cool down an additional cooling fluid, which is often a silicon oil. The term thermal fluid is used for the second stage cooling fluid and it differs to the refrigerant, because it does not change its phase. The thermal fluid remains in liquid form and is therefore also safer to handle, as it does not escape as gas. The thermal fluid works as heat exchanging medium. It is pumped through an external circulation between the cooling unit and the to cooled object. The thermal fluid absorbs the heat of the to cooled object and emits the heat to the refrigerant. The thermal fluid can also be heated by a heating element. This process is also shown in Figure 3.1. [51] The circulation between cooling unit and the to cooled object is often realised by cooling hoses and some kind of heat exchanger. A heat exchanger can be a cooling coil around the object, a heat sink direct at the heat source, or internal cooling ducts, where the thermal fluid flows through. The temperature of the thermal fluid directly after it leaves the cooling unit is called supply temperature. In cooling process it is the coldest stage of the thermal fluid. During the transport though the hoses the thermal fluid absorbs heat from the environment and at the heat exchanger it absorbs heat from the to cooled object. The temperature directly before the cooling unit is called return temperature and is of course higher than the supply temperature. The cooling unit tries to decrease the return temperature of the thermal fluid to supply temperature level. But this is only possible if the

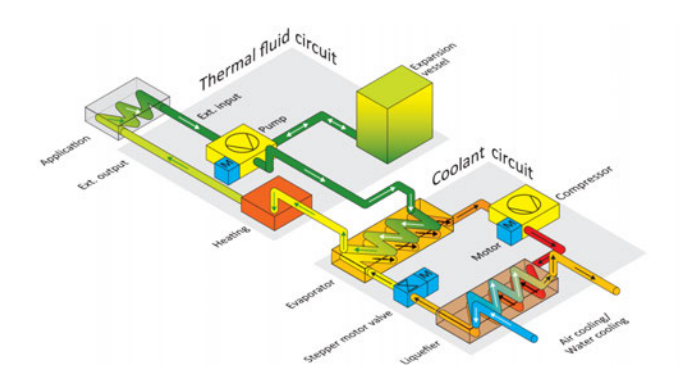


Figure 3.1: Working principle of a cooling unit [51]

maximum cooling capacity is not exceeded. The cooling capacity is the amount of heat, which can be extracted from the thermal fluid by the refrigerant within a second. Is the temperature difference between supply and return temperature or the mass flow of the thermal fluid too high, the thermal fluid can not be cooled to the desired supply temperature. The actual supply temperature rises. Insulation can be used to reduce at least the heat absorption from the environment, this heat share is also called cold losses. The characteristics of the heat exchanger also influence the required cooling capacity. The higher the distance between cooling target and thermal fluid, the higher must be the cooling capacity and the lower must be the required supply temperature, as the heat must travel at first through more material, until it arrives the cold thermal fluid. With a higher mass flow, the thermal fluid can extract more heat from the target object, but must also emit more heat to the refrigerant.

As shown in Figure 3.2, cooling units can also deliver constant heat capacity, but the cooling capacity depends on the supply temperature. The lower the temperature, the lower the cooling capacity. This has following reasons: inside the vapor compression cycle the compressor must lift the temperature of the refrigerant over the ambient temperature to emit the previously absorbed heat to the environment. With a low supply temperature the difference to the ambient temperature is much higher compared to a medium supply temperature. The necessary temperature to emit the total amount of heat is even higher. A higher compression of the refrigerant will be needed, which causes higher power consumption or surpasses the capabilities of the compressor. Since the compression ratio is limited, the system will not absorb any more heat, if the capacity demand exceeds the capacity limit. Therefore the cooling capacity will decrease.

The extracted heat by the refrigerant and also heat losses from compressor and pump must be removed from the cooling unit. This can be done by air cooling, where the cooling unit is

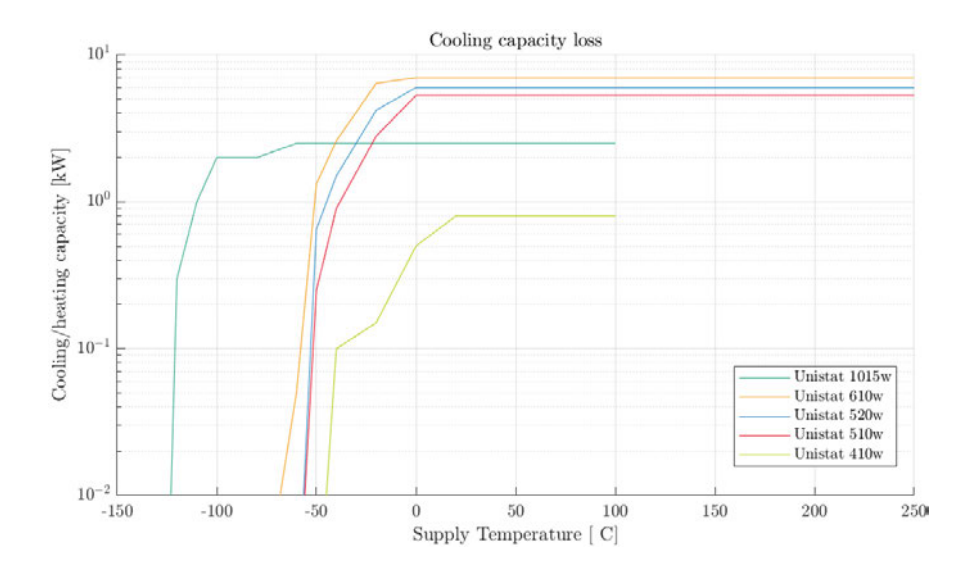


Figure 3.2: Cooling capacity loss of cooling units from manufacturer Huber [50]

cooled by the surrounding air in the room thus the air temperature in the room will increase. The cooling unit needs a heat sink and a ventilation, which will make the unit bigger and increases the noise in the room. A cooling unit can also be cooled by circulating water. The cooling unit is connected to an external water cycle. The water flows through the connection of the unit and absorbs the heat loss of the unit. The water must be cooled down at a central cooling station, for example another cooling unit on the roof. In contrast to the primary cooling unit which reaches the very low target temperatures, such a cooling unit can operate at much higher environmental conditions. But the necessity of a pump system and building water pipes to the target location increases the installation effort.

Cooling units are available with temperature limits down to -120 $^{\circ}$ C with a cooling capacity of 300 W at this temperature [50]. At higher temperatures, higher cooling capacities are possible. In example the same unit has a cooling capacity of 2000 W at -100 $^{\circ}$ C. Another unit only reaches -60 $^{\circ}$ C but with a cooling capacity of 3000 W [23].

Climate chambers

In climate chambers, the vapor compression cycle is used to directly cool down the air inside the chamber. As the air is the cooling medium, climate chambers are not only insulated to the surrounding environment, but also air sealed. For very low temperatures under -40°C an additional cooling stage may be needed [58]. Two vapor compression cycles are serially

connected, so the first stage reduces the environment temperature for the second stage and enables the low temperature after the second stage. High temperatures can be achieved using electric heating elements. A ventilation system distributes the heated or cooled air evenly in the test room to ensure constant temperature at every point on the surface of the test object, shown in Figure 3.3 [58]. In general, climate chambers are used, to investigate the behavior of products at low temperature or to ensure that products work safe at various temperature and air conditions. That is why they are often equipped with humidifiers and dehumidifiers. Humidifiers emit vaporised water into the circulation air flow to increase the humidity. A dehumidifier decreases the humidity. A cold surface inside the air flow forces the air to condensate. The resulting water is collected externally.

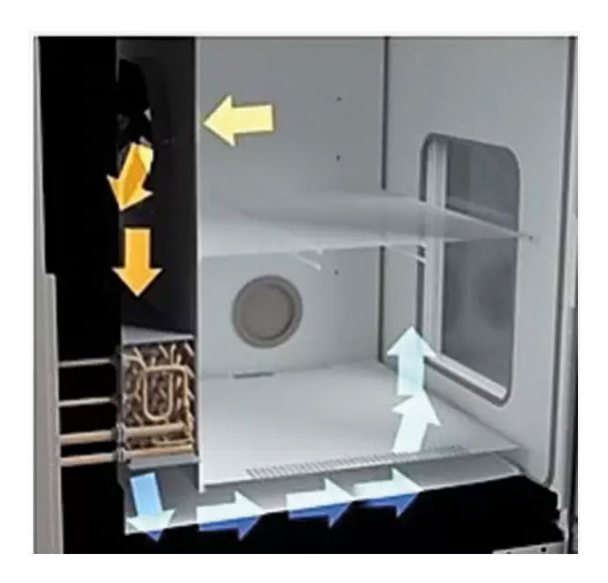


Figure 3.3: Air flow inside a climate chamber [58]

There are also other chamber designs. Instead of a vapor compression cycle inside the chamber, the chamber interior is wrapped with a fluid coil, where the thermal fluid of an external cooling unit flows through. The chamber itself accomplishes the purpose of an insulated box. The layout is shown in Figure 3.4. The absence of any electrical or rotating device disallows the control of humidity but reduces the influence of magnetic radiation or vibration. According to a study of the Ilmenau University of Technology, a very high temperature stability can be achieved with this design [26].

Some climate chambers have openings in their wall to allow cable routing. Cables may

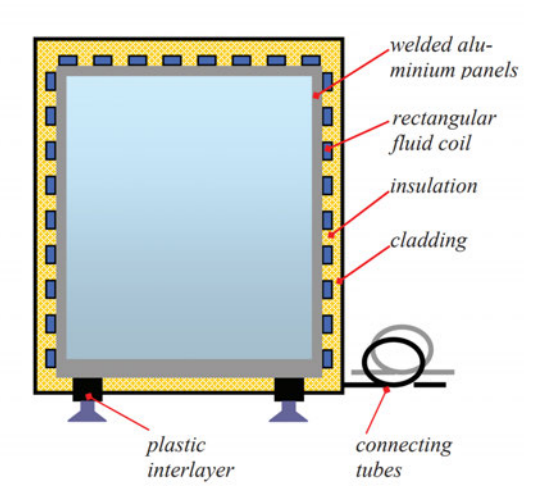


Figure 3.4: Cross sectional view of climate chamber from the TU Ilmenau [26]

be needed for sensors or motor control. This openings are a blind spot for the insulation. To prevent convection and air exchange from outside the openings have seals for required cable diameter.

Climate chambers are available in various sizes, from tiny cabinets for investigating biological cell behavior to big halls for testing vehicles. The interior climate is controlled and regulated from the outside. The temperature ranges can go from -80°C to +360°C [38] with a temperature stability up to \pm 0.1 K [7]. The relative humidity can be regulated from 10 % to 98 %[7].

3.1.2 Cold by phase change

When a substance changes its phase from gaseous to liquid, or from liquid to solid, it emits heat, which is called heat of condensation and heat of evaporation. A phase change in the other direction, from solid to liquid and from liquid to gaseous, requires energy. This energy is extracted from the environment in form of heat. The extracted heat causes a temperature decrease. This effect can be observed on gas cylinders if a lot of gas has been extracted or on ice inside a glass which cools the liquid while melting. The cooling process holds a constant temperature and lasts until the substance is completely converted to gas. Some substances have very low boiling or sublimation points, which make them useful for cooling applications. These substances are called cryogens. Common cryogens are liquid nitrogen (-196 °C boiling point [9]) or dry ice (-78.5 °C sublimation point [9]). For cooling applications, the object to

be cooled is doused into a container filled with a cryogen. The phase change of the cryogen allows it to hold a constant temperature, but for controlled temperatures other applications are needed. Specific temperature can be achieved by controlling the amount of cryogen, which is injected into an insulated system.

3.1.3 Thermo electric effect

In 1834, Jean Charles Athanase Peltier discovered that when an electrical current flows through two semiconductors with different energy levels, a temperature difference and therefore a heat flow is created at the junction. Electrons which flows from the semiconductor with lower energy level must increase their energy level to pass the junction and to enter the semiconductor with higher energy level [8]. This happens by absorbing heat. When the electric current direction is switched, the electrons from the semiconductor with higher energy level have to lower their energy by emitting heat. This phenomena is called Peltier effect. It is the reversal of the earlier discovered Seebeck effect, where electricity is produced by delivering a temperature difference [32]. The working principle of both effects is shown in Figure 3.5.

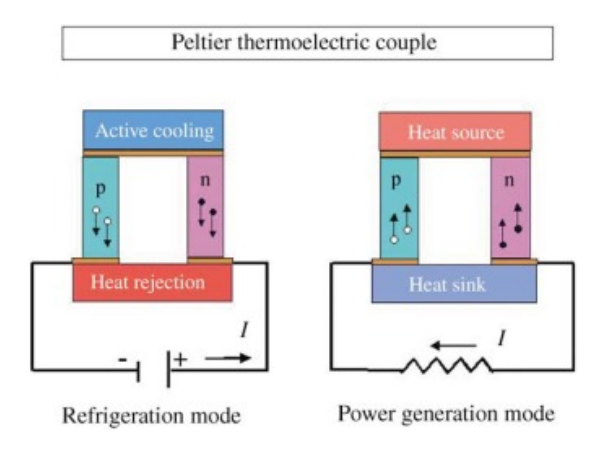


Figure 3.5: Working principle of Peltier (left) and Seebeck (right) effect [63]

The Peltier effect of a single junction generates a very small temperature difference. For the use in industrial applications multiple of those semiconductor couples are stacked in a row. They form a Peltier element. Commercial available Peltier element and its layout is shown in Figure 3.6. The temperature difference and therefore the heat flow increases in proportion to the electrical current. As the heat loss due to the line resistance increases squared to the current, the cooling efficiency decreases with increasing temperature difference. If the current is too high, the cooling capacity drops. To retain high cooling capacity, an additional cooling for the heat rejection side is used. An other strategy to reduce the individual temperature

difference is to stack multiple Peltier elements on top of each other as shown in Figure 3.6. Peltier elements can be directly applied on the surface of the to cooled object, or they can be

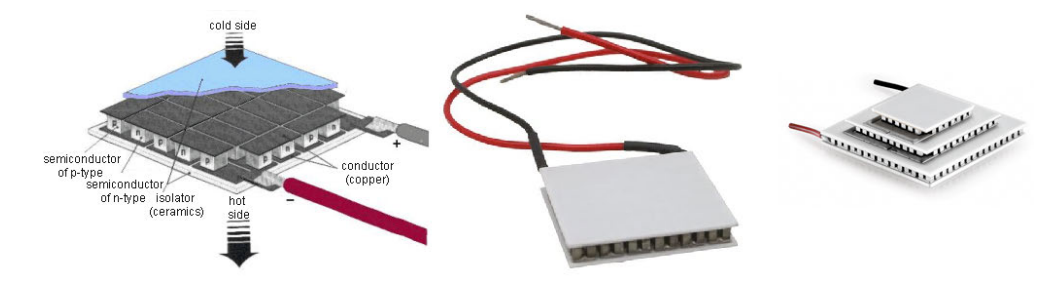


Figure 3.6: Common Peltier element (left, middle) [35] and a multi-stage Peltier element (right) [61]

used to cool down the air around the object. Both sides are then equipped with a heat sink and a fan, to allow an efficient temperature distribution. The principle is used in some climate chamber designs and is visualized in Figure 3.7.

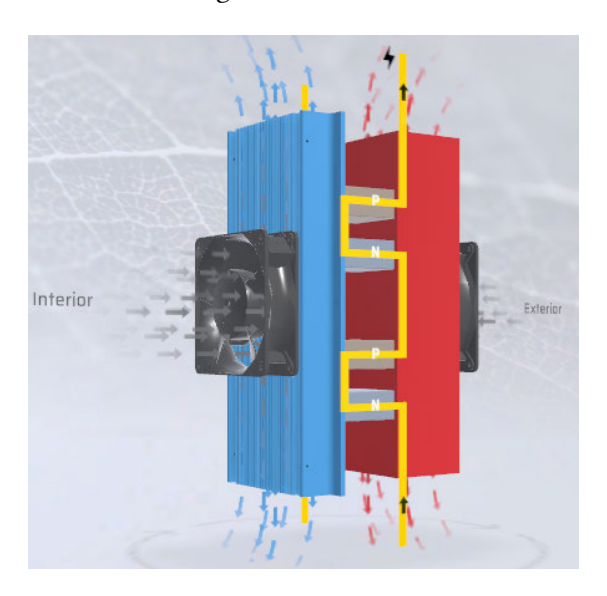


Figure 3.7: Peltier cooling element for climate chambers [24]

3.2 Materials

The efficiency of cooling systems is often effected by the used materials for insulation against cold losses and conduction for a good heat transfer. In the following a collection of materials for insulation and conduction purpose are introduced.

3.2.1 Thermal conductive materials

These materials are used to maximize the heat transfer. In general, metals have a good thermal conductivity, as the molecule structure allows a good energy distribution. For some applications, flexible materials with a high conductivity are needed. In this case, thermal interface materials (TIM) like heat pastes, gap fillers or gap filler pads are used. Heat pastes usually are a blend of metal particles and oil, which are mostly used in the chip industry. Gap fillers are pastes or foam pads, which are used to bridge small distances or unevenesses. They are often made of a silicon elastomer with metal ceramic particles [22]. The thermal conductivity of metals depends strongly on the temperature. Common conducting materials are listed in Table 3.1.

Table 3.1: Collection of thermal conducting materials

Type	$\frac{1}{k\left[\frac{W}{mK}\right]}$
Metal	220 [46]
Metal	380 [46]
TIM	2-6.5 [21]
TIM	1.1-50 [21]
TIM	2-6 [12]
Metal	46.5 [46]
N N	Metal Metal FIM FIM

3.2.2 Thermal insulation materials

The goal of insulation is to reduce the heat transfer. In the field of insulation, the term specific thermal resistance is also used. It is the reciprocal of the thermal conductivity, the higher thermal resistance the lower thermal conductivity. The absolute thermal resistance refers to a defined geometry [60].

As mentioned in Section 2.2 heat transfer consists of heat conduction, heat convection, and thermal radiation. Insulating materials constrain a reduction of at least one of those modes. Mainly convection is reduced, which is achieved by trapping the air in tiny pockets inside the material. Gasses have a low conductivity in general, but transport heat by convection very



Figure 3.8: Flexible synthetic rubber (left), insulation bag (middle), and vacuum insulated panels (right)

well. By restricting the flow freedom of the air molecules to small regions, convection can not happen on large scale, which reduces the conductivity of the entire material. [59]

Common insulation materials and their thermal conductivities are listed in Table 3.2. As

Table 3.2: Collection of thermal insulating materials

Material	Type	$k\left[\frac{W}{mK}\right]$	Available shapes		
Aerogel	Superinsulation	0.017 - 0.04 [1]	Mats		
Cellulose	Organic	0.04-0.05 [18]	Boards, mats, filling material		
EPS	Organic	0.029-0.041 [34]	Boards, solids		
Glass wool	Inorganic	0.03-0.046 [66]	Boards, mats, filling material		
MDF	Organic	0.107-0.123 [52]	Boards		
OSB	Organic	0.098-0.106 [52]	Boards		
Plywood	Organic	0.158-0.173 [52]	Boards		
PU Foam	Organic	0.02-0.027 [34]	Boards, solids		
Synthetic Rubber	Inorganic	0.032-0.039 [30]	Mats		
Textile waste	Organic	0.044-0.103 [5]	Filling material		
Vacuum insulated panels	Superinsulation	0.004-0.008 [19]	Boards		
XPS	Organic	0.025-0.035 [34]	Boards, solids		

already mentioned in Table 3.2, insulation materials come in various shapes and forms. Some of them are shown in Figure 3.8.

3.3 Existing test rigs with temperature systems

3.3.1 Test rig of Mannheim Tribology Competence Center (KTM)

The Oscillating Rolling Wear Test Bench at the KTM investigates wear protection behavior of lubricating greases in rolling element bearings. The test rig is designed for small swivel angles from 0.2 to ± 1.3 and the use of 51206 thrust ball bearings [31]. The swivel movement is achieved by an eccentric tappet at a electric drive and a connection rod to the bearing. The bearing can be loaded with 100 to 8000 N by a disc spring. A common test on this test rig is

the SNR-FEB2 standard tests for greases in wind turbine applications. In this test the bearing is loaded with 8000 N and executes swivel movements of \pm 0 at 25 Hz [27]. The test runs for 50 hours usually at room temperature or at \pm 20°C. After the test is finished, the bearings are weighted and visually inspected. The test rig is shown in Figure 3.9.



Figure 3.9: Oscillating Rolling Wear Test Bench of KTM [31]

A heat sink which lays directly under the bearing enables the low test temperature. It includes internal cooling ducts, where the thermal fluid can flow through. The thermal fluid is supplied by a cooling unit. The test rig can also be heated up to 80°C. The cylinders in Figure 3.10 are used as insulation. The test rig is screened by an aluminum rack with windows made of Plexiglas. The interior is supplied with nitrogen to reduce icing.



Figure 3.10: Cylindrical cover to insulate the bearing [31]



Figure 3.11: Test rig of the IMKT [17]

3.3.2 Test rig of Institute of Machine Design and Tribology (IMKT) at Leibniz University of Hanover

This test rig investigates the influence of the contact geometry on fatigue behavior of oscillating rolling element bearings. It is designed for radial and axial rolling element bearings from 20 to 60 mm in diameter. The maximum swivel angle is \pm 0 at a frequency up to 30 Hz. The bearings can be loaded with up to 50 kN axial and 20 kN radial. They can be lubricated in various forms: injected oil, plunged oil, grease, and dry lubricant [17]. On Figure 3.11 a schematic section view of the test rig is shown. The shaft in the middle is connected to a motor. The bearings are mounted on the shafts left and right.

The bearings can be cooled down to almost -20°C. Therefore cooling ducts are inside the bearing seats. A cooling unit pumps thermal fluid through the cooling ducts. The cooling unit has a supply temperature of -20°C and delivers 1.2 kW cooling capacity at this temperature. It is covered by insulation blankets to reduce icing and heat transfer.

3.4 IWES test rig BEAT0.2

The test rig BEAT0.2 (Bearing Endurance and Acceptance Test Rig, second test rig for bearings under one meter in diameter) was build to investigate wear protection characteristics of greases and blends of greases under comparable conditions as pitch bearings of wind turbines but with low test execution costs and short bearing exchange duration. Due to the fact that pitch bearings nowadays have a diameter of six or more meters, causing tons of weight, they are not easy to handle. Therefore a scaled principle was developed to allow the use of standard ball bearings for expressive test results.

3.4.1 Scaling of real wind turbine pitch conditions for pitch bearings

Stammler 2020 mentioned in his work that mostly the contact pressure and the relative travel distance of the rolling elements influence wear behavior [55]. A reference parameter can be determined from this: $\frac{x}{2b}$, where x is the relative travel distance of a rolling element and 2b the width of the Hertzian contact ellipse (shown in Figure 3.12). When the pitch angle increases, x also increases, the same applies to contact pressure and 2b.

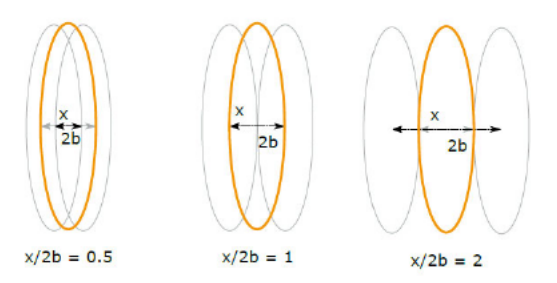


Figure 3.12: Visualization of x/2b ratio [55]

Stammler summarized following requirements for a scaled bearing test: the contact pressure and the rotation frequency has to be close to full scale, kinetics and kinematics similar to full scale, and $\frac{x}{2b}$ and lubricant identical to full scale scenario [55]. Two angular contact ball bearings create a similar contact situation as four-point contact ball bearings which are used for real pitch bearings. Figure 3.13 shows the similarities.

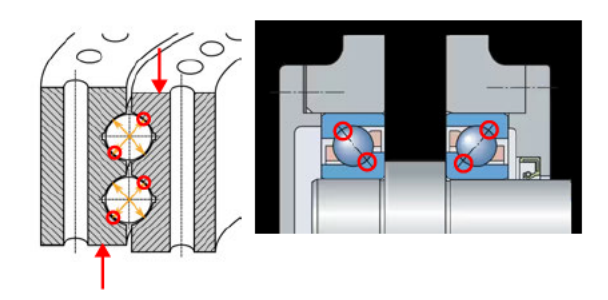


Figure 3.13: Four-point contact ball bearing (left)[20] and two angular contact ball bearings in x-configuration (right) [13]

Bartschat et. al. [2] used aeroelastic simulation data of the IWES IWT-7.5-164 Reference Turbine [36] and site-specific wind speed measurements to develop a test program which consists of 13.7 h of wear-critical pitch bearing operating conditions. Due to the stochastic nature of wind speeds and the characteristics of the pitch controller, the test program is characterised

by oscillating movements with variable amplitudes and static loads. Figure 3.14 shows the resulting distribution of the amplitude ratios x/2b for the test program.

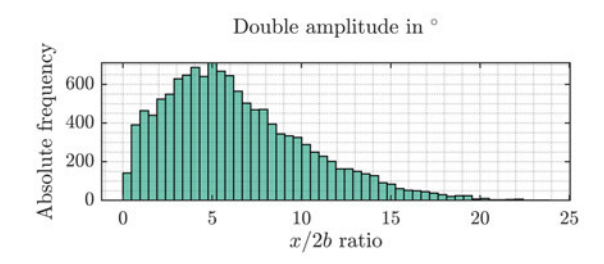


Figure 3.14: x/2b amplitude ratios of IWES IWT-7.5-164 Reference Turbine [2]

3.4.2 Layout of the test rig

The test rig is pictured in Figure 3.15. The computer controlled electronic drive executes a specific oscillating rotation pattern. The resulting torque is measured with the torque meter. The torque is forwarded to the shaft inside the bearing housing. The bearing housing includes two 7220 angular contact ball bearings in x configuration, a pressure plate, and a hydraulic cylinder. The hydraulic cylinder produces 90 kN of axial load to the pressure plate which distributes the force on the outer ring of the back bearing [2]. In addition to the torque, the temperature of the back bearing and the pressure inside the hydraulic cylinder are measured, too. The hydraulic pressure is not regulated by a computer. The pressure must be adjusted manually by using a hand pump. The sensor data is transferred to a database where it is saved to a respective test id. All components are mounted on a groove plate of steel. Bellow couplings connect the drive with the torque meter and the torque meter with the shaft to compensate axial and radial offset.

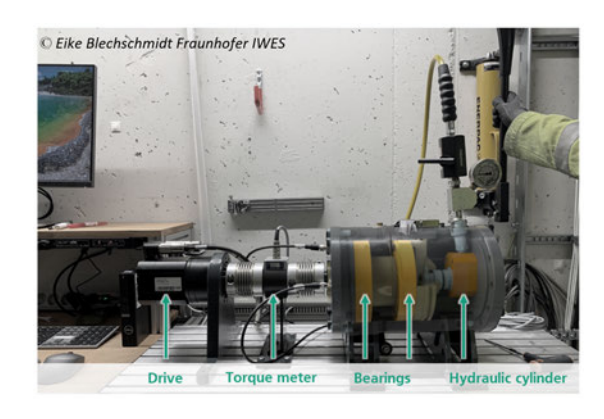


Figure 3.15: Layout of BEAT0.2 test rig [2]

To change the bearings the shaft must be detached from the bellow coupling. With loosed bolts on the feet mount, the housing can be pulled backwards. Turned to the front, the front plate of the housing can be detached. The shaft with the bearings can be pulled out of the housing. The shaft is clamped into a vice where the bearings can be dismounted by mechanical jaw pullers. New bearings must be heated with an induction plate, so they fit on the bearing position of the shaft. Lubricated with fresh grease the bearings on the shaft are mounted as previously described but in inverted order. In Figure 3.16 the shaft without bearings is shown next to the housing.



Figure 3.16: Shaft without bearings next to drive, torque meter and housing

3.4.3 Analysis of results

After the test is completed, both bearings are cleaned and the raceways of the inner ring are visually analyzed. If there is any damage, the damage types and wear mechanisms are compared to other test results with different greases or a different grease blend. If necessary the friction torque can be accessed via the database for further investigation.

4 Low temperature tests with a rented cooling unit

Fraunhofer IWES has rented a cooling unit to investigate whether the test rig withstands the low temperatures. It has also been tested, which temperatures can be achieved with the chosen cooling unit. Its specifications are listed in Table 4.1. A 18 mm diameter copper tube with a thickness of 1 mm has been wrapped around the housing as a cooling coil to extract the heat energy of the test rig. The changes to the housing and other adaptions are explained in Section 4.1. As the exchange handling of the bearing is an important criteria, the work flow and encountered difficulties were noted and are explained in Section 4.2 and 4.4.

Table 4.1: Specification of the rented cooling unit

Specification	Value			
Temperature limits	-50°C to 250 °C			
Heating capacity	6 kW			
Cooling capacity	see Table 4.2			
Max. volume speed rate	112 l/min			
Pump speed region	1500 rpm to 6000 rpm			

Table 4.2: Cooling capacity of the cooling unit

Temperature [°C]	-50	-40	-20	0	20	100	200	250
Cooling Capacity [kW]	0.25	0.9	2.8	5.3	5.3	5.3	5.3	5.3

4.1 Changes of layout and insulation

As there are two bearings it would have been natural to use two coils, so the temperature profile in the cooling coil would not cause different temperatures at the bearing. But putting two coils next to each other would have resulted in an unused gap between the return part of the first coil and the supply part of the second coil. That is why only one cooling coil has

been used. The coil has been wrapped 8.5 times around the housing. The first stand has also been replaced by a thinner wood stand, which has been moved under the front panel, to gain extra space. Finally, these changes have achieved a much higher from the coil covered area, especially around the bearing position. The copper tube wrapped around the housing is shown in Figure 4.1.



Figure 4.1: Copper coil wrapped around the housing

Every sensor hole, which were not in use, has been closed with tape to prevent air circulation. An acrylic glass plate of 5mm thickness and a wood plate with a thickness of 15 mm has been placed between the aluminum and the feet of the test rig to improve the insulation to the ground. The housing has been additionally covered in insulation material, which was put as tight as possible around the surface, to reduce the amount of locked in air. The amount of insulation layer varies between 1 to 3 layers with a layer thickness of 10 mm each. The coupling has also been insulated with a single layer of insulation material, after it has been noticed, that the icing at this area was very heavy (Figure 4.2).

The added insulation has caused a rise of friction, as it has rubbed against the insulation of the front panel, but this rise has been relatively small in comparison to the friction torque in the bearing. The supply and return cooling hose have been already insulated with 10 mm thickness, but additionally 20 mm insulation at straight regions and 10 mm at curved regions have been added, after condensate has been noticed. Blocking valves were placed between supply hose and cooling coil, and between return hose and cooling coil. The valves were insulated with T-piece pipe insulation and straight pipe insulation was imposed over the levers



Figure 4.2: Ice around coupling and shaft

as shown in Figure 4.3. The insulation has been fixed with laces and tape. The final insulated test rig is imaged in Figure 4.4.



Figure 4.3: Insulation of the valves

4.2 Bearing exchange work flow

Usually the bearing exchange can be started directly after the end of the test sequence. But the cooled test rig must be unloaded and defrosted at first. The unit itself can accelerate this process by heating the cooling unit. The duration of the process depends on the cooling temperature. Removing the insulation can also accelerate the defrosting process, but will



Figure 4.4: Insulated test rig

also increase condensate, as the humid air of the room has access to the cold test rig surface. With closed insulation and heating support from the test rig, the defrosting time numbers to 2 hours. After defrosting a part of the insulation must be removed to get access to the bolts. This process took 5 minutes on average. It was necessary to proceed more carefully, as the original stand was replaced by a wooden stand that was less stable. While moving the housing, a second person was needed to stabilize the wood stand. At first, the movement was supported by a crane, to prevent damage to the copper coil due to a forward tilt. But it was noticed later, that a foam mat under the copper coil provided sufficient protection. The shaft could then be pulled out. The process of disassembling the bearings from the shaft, and cleaning, assembling, and lubricating new ones does not differ from the usual procedure. With pushing the shaft into the housing and assembling the front panel, the procedure takes one hour in average. The positioning of the housing turned out to be complicated, as the wood plate has blocked the sight on the groove stones. The cooling hoses also reduce the freedom of movement of the housing. This limitation of movement cost around 5 additional minutes for the positioning. Putting the insulation back on took 20 minutes on average. Then the cooling process can be started. The necessary time for reaching the target temperature depends on the temperature. 45 minutes were needed to start at 27°C and reach 0°C, but additional 45 minutes were necessary until the process temperature was constant. The achievement of -10°C took around 1.5 hours and after an additional hour the temperature was constant, but the controller setup of the unit was not optimal, so a faster cooling time should be possible. The change of the controller setup between the tests makes the comparison of the cooling time difficult. The work steps, required time, and required numbers of workers are listed in Table 4.3. As

already mentioned, the cooling time and also the defrosting time depend on the target process temperature.

Table 4.3: Changed work steps for low temperature tests

Step	Description	Time	Number of workers	Change
1	Assembling of the bearings	1 h	1	
2	Positioning of the housing	5 min	2	1 additional worker
3	Assembling of the housing	5 min	1	
4	Attaching insulation	20 min	1	new
6	Cooling	1.5 to 3.5 h	0	new
7	Applying the load	5 min	1	
8	Test	13,7 h	0	
9	Removing load	1 min	1	
10	Defrosting	2 h	0	new
11	Detaching insulation	5 min	1	new
12	Disassembling of the housing	5 min	1	
13	Positioning of the housing	5 min	2	1 additional worker
14	Disassembling of the bearings	30 min	1	

4.3 Test results

Nine tests with four different greases were done in total. Every grease was tested at 0°C and -10°C. One grease was also tested at -10°C with 10% water additive. Stammler [56] has explored, that already at 0°C an increase of the friction torque in comparison to room temperature is noticeable in almost every cases. One single grease has shown an abnormality. The friction torque at -10°C was lower than at 0°C. For a valid predication, the test should be repeated, but current test results indicate the importance of low temperature tests.

4.4 Acquired knowledge

The first test was started at a bearing temperature of -20°C. This temperature caused very high friction torque and the drive stopped the test procedure to prevent damage. For future tests at those temperatures, the drive and the torque meter have to be replaced by components, which withstand higher torque. This limitation is also the reason, why there was no test made at lower temperatures.

It was investigated, that the tighter the insulation sits on the surface, the less icing appeared.

Less icing also caused faster cooling. In general the amount of ice at the surface was higher than expected. It is very likely, that the insulation did not prevent the air to reach the surface of the test rig. This effect could be minimized by building an air tight box around the test rig. The internal air will still cause icing, but the amount of possible icing is limited to the absolute humidity inside the box.

When the test rig was heated up to room temperature, the frozen condensate melted. The water was not directly absorbed from the air, so it stayed on the painted metal surface of the test rig. Over time, the paint came off and the blank metal surface started to rust. It is likely, that the paint was not designed for these temperature changes.

The shape of the insulation was cut out of the insulation material roll. The borders were masked with tape, but the process of putting the insulation off and on caused cracks. This worsened the insulation. Damaged insulation pieces were replaced, but at future tests, a more durable insulation solution should be designed.

During the cool down, the pressure inside the piston decreases and with it the axial load. To load the bearing with the desired force, the test rig must be loaded, after the target temperature is achieved. It also must be unloaded, before the heating process starts, because the temperature increase causes a pressure increase. The pressure could overstep the breaking point of the piston. Loading and unloading has so far been done by a hand pump, that means that it has been necessary to wait until the cool down process is finished. An automated pressure control would reduce the work effort, because an external actuation would not be necessary.

The bending of the copper tube around the housing was possible, but a constant contact could not be achieved. This lead to partially large gaps between the cooling tube and the housing. The circular cross section is also adverse for the heat transfer. During the cooling process icing was noticed in the gaps. The use of gap fillers, heat paste, or a rectangular tube will probably increase the cooling efficiency.

It is possible to cool down the temperature at the bearing below -30°C with a cooling unit which provides -50°C supply temperature and 250 W cooling capacity. Unfortunately the power consumption was not measured.

5 Evaluation of temperature systems

As there are different possibilities to cool down a test rig, a selection of temperature systems will be compared to each other. The advantages, disadvantages, from the author recommended changes to the housing and required components will be described. The following criteria are used to evaluate the system and are rated in accordance with VDI standard 2225 [65] as ideal, good, sufficient, acceptable, and unsatisfying.

- Estimated investment costs: Costs of the temperature system, necessary changes to the test rig, and required equipment. Ideal means very low costs.
- Estimated operating costs: Costs during the tests like rent, power consumption, etc. Ideal means very low costs.
- Inconvenience of bearing exchange: Negative effect on the bearing exchange workflow. Ideal means very low inconvenience.
- Estimated space requirements: Dimensions of the system, building-side connections. Ideal means very low requirements.
- Hazard: Possible dangers during the bearing exchange or cooling process for workers and environment. Ideal means very low dangers.
- Flexibility: Access restrictions and alternative use cases for the temperature system. Ideal means very high flexibility.
- Cooling performance: required time for cooling process. Ideal means very low required cooling time.
- Automation capability: Possible integration into the computer controlled system and availability of an interface for additional temperature sensor as control variable. Ideal means very high automation capability.

All of the following temperature systems are capable of heating, so this is not an evaluation criterion. Climate chambers and cooling units both benefit from a water cooling system.

Therefore, it is not included in the investment costs. Cryogens were mentioned in Section 3.1.2, but will not be considered in the evaluation.

5.1 Climate Chambers

As already mentioned in Chapter 3.1.1 some companies have their own climate chambers to test their products. To increase the usage they hire out time slots to external customers, so the customers can test their products without the need of an own climate chamber. There are also companies, which have specialized on climate chamber space renting.

At first the required space has to be determined. This depends on the components besides the bearing housing which are inside the chamber, and the necessity of placing components in the chamber depends on the layout of the chamber itself. If there are openings at the right position, then there are multiple options. If the climate chamber has an opening for the rotating shaft, only the bearing housing must be inside the chamber. If the opening is just big enough for the power, control, and measurement cables, the complete drive train, consisting of the drive and the torque measurement shaft, must be inside. With internal power supply, the control cabinet including data storage and computer could also be placed in the chamber, but at least one opening is necessary for the hydraulic tube. The hydraulic cylinder is admittedly equipped with a valve, which can be closed, after loading and before entering the chamber or starting the cooling process. But the tests in Section 4 have shown, that the pressure is heavily effected by the temperature. The hydraulic tube must be routed through the wall, so the hand pump can be actuated from the outside, when the target temperature is achieved. Instead of a manual hand pump, a hydraulic unit could be placed inside the chamber and be connected to the control cabinet for an automated actuation. Then there is no opening needed, but the hydraulic unit must withstand the conditions inside the chamber. The necessary space can be calculated by determining the smallest cuboid, where all the components in working position fit next to each other on the ground like in Figure 5.1.

It is assumed, that most rentable climate chambers will have some kind of opening, as the customers usually have their own measuring system. This will allow a placement of the control cabinet and the hydraulic hand pump outside of the chamber. But a matching opening for the shaft is unlikely. At least the drive and the torque meter must withstand the conditions inside the chamber. For example the drive has a temperature range where it works optimal. Outside of this range the torque may not fit to the characteristic curve which is implemented in

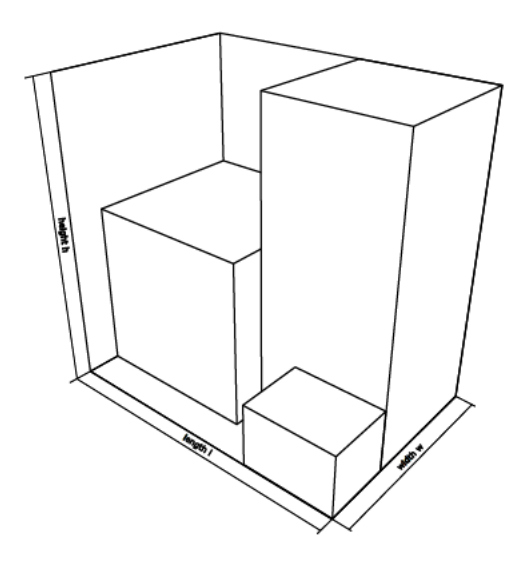


Figure 5.1: Schematic of smallest cuboid

the control system. In the worst case the extreme temperatures cause fatal damages to the drive.

The investment costs are limited to the purchase of components intended for the temperatures. The rental of climate chambers is calculated per commenced day [3]. If 14 hours test duration and cooling and heating time are to be agreed with normal working hours, then at least two days are necessary. With transportation of workers and test rig high operation costs are expected. The lack of availability of the own workshop increases the inconvenience of a bearing exchange. But instead there is no space on own property needed and the institute is not responsible for any maintenance. Any safety risks are rated as low, as the chamber is probably operated by trained professionals. The climate chamber will cool down the air around the test rig first, which is a realistic simulation of real conditions. The control of humidity is another advantage.

Temperature system: 1 Investment cost: Ideal

Operating costs: Unsatisfying

Inconvenience of the bearing exchange: Unsatisfying

Estimated space requirements: Ideal

Hazard: Ideal

Flexibility: Unsatisfying

Cooling performance: Good

Automation capability: Unsatisfying

One of the biggest disadvantage of a rented chamber slot is the dependency to free time slots and the haul to get the test rig to the climate chamber's operating company. When there is a regularly demand on tests at low temperature, it can be more sensible to buy an own climate chamber. This chamber can be adapted to the most necessities. To minimize the chamber dimensions and any exposure of the equipment, it is useful to place only the housing inside the chamber. So the drive and the electric cabinet can operate at room temperature. Openings are required for cable routing, and the shaft. The support inside the chamber must carry the weight of the housing with all interior parts. The total weight amounts to around 100 kg. The chamber can be equipped with draw runners, so the support can be pulled in direction of the door to ensure an uncomplicated bearing exchange. These draw runners must be locked during the test, to avoid axial mismatch caused by vibrations. The cables and tubes must be long enough, so they do not rip while pulling the support. The support can only be moved, when the coupling is not connected to the shaft. This can be achieved, when it is possible to pull the complete drive train away from the climate chamber or vice versa. An alternative is to place the housing in a position, where the shaft shows in the direction of the door. The opening for the shaft must be inside the door too. The shaft with the bearings can be pulled through the open door, without the need of moving the housing. A climate chamber with a lot of adaptions will increase the investment costs to around 40 000 to 50 000 €. But due to the good insulation, the operating cost will probably be low. A disadvantage in comparison to cooling units is, that the chamber must be placed directly at the test rig, however the safety is higher. Modern climate chambers allow an integration in existing control systems.

Temperature system: 2 **Investment cost:** Acceptable

Operating costs: Ideal

Inconvenience of bearing exchange: Good **Estimated space requirements:** Acceptable

Hazard: Ideal

Flexibility: Acceptable

Cooling performance: Sufficient **Automation capability:** Ideal

5.2 Cooling unit solutions

Commercial cooling units are available in various temperature and capacity ranges. They do not need any complex installation after the delivery. The effort and efficiency for this application is given by the location of the cooling duct. In the following six different solutions are explained. The automation capability does not differ between these solutions, as it mostly depends on the cooling unit. Cooling units can be integrated into an external control software system, and have an interface for additional temperature sensors, so for every cooling unit solution it is rated with high. The flexibility for cooling unit solutions is generally rated with medium to high, because the cooling unit can be used for other experiments and the institute owns it. Cooling units usually have an heating option, therefore it is rated as high. The unit itself can cost around 35 000 ϵ and an insulation is necessary, which justifies the investment costs rating as at least medium. The operating costs are rated in general as medium, but it depends on the power consumption dependent on the cooling capacity and the frequency of the thermal fluid change.

5.2.1 Cooling ducts inside the bearing seat

The required supply temperature increases with increasing distance to the target location. Therefore the most efficient solution is to place the cooling ducts as close to the bearing as possible. A cooling tube made out of copper can be placed inside a groove at the bearing seat, so the tube is in contact with the outer ring of the bearing. However, this does not provide a sufficient contact surface for the outer ring. A reduced support area would increase the contact pressure of the outer ring and this could lead do damage. An alternative is to place cooling ducts inside the bearing seat. The cooling duct will not have direct contact to the bearing, and the heat conduction trough steel is worse than through copper. But it still will be in near proximity of the bearing and the support for the outer ring will not be compromised. Quick couplings or valves at the housing could connect the cooling hose from the cooling unit with the cooling ducts inside the housing. As there are two bearings, it must be considered, whether the cooling lines are in serial, or parallel. A serial layout would have the advantage, that there are only one inlet and one outlet at the housing. But the temperature of the thermal fluid at the second bearing position would be higher than at the first position, due to the absorption of heat along the way. A parallel layout requires two inlets and two outlets and also a T-piece adapter for supply and return cooling hose, but will provide equal temperatures at each bearing. Both layouts are shown in Figure 5.2.

This solution requires the machining of a new housing. One machining possibility would be

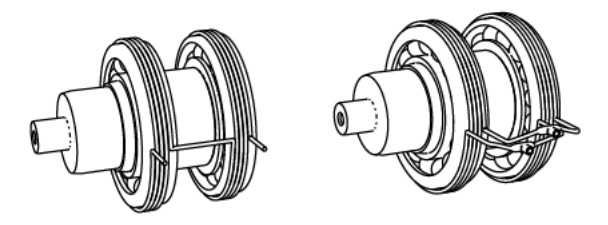


Figure 5.2: cooling ducts in serial (left) and parallel (right)

to split the design of the housing in a top and bottom part and creating rings for the bearing seat. The rings have a spiral profile on their outside, where the thermal fluid flows through. The internal profile of the top and bottom side can be milled with some extra material left for precise lathing, but the contour for the cooling duct rings inside the bearing seats and also the holes for the inlet and outlet must be finished. The form of the rings or the contact pressure must keep the thermal fluid inside the ducts. The position can be fixed by cylindrical pins. After the rings are in place, the top side can be mounted on the bottom side. A final lathing procedure of the inside provides a total concentricity. Steel on steel does not provide a perfect tightness against fluids. As the pressure of the fluid is already limited by the pump of the unit (the rented unit in Section 4 has its limit at 1.5 bar), the tightness might be sufficient, but it may be useful to integrate some flat seals between the top and bottom part, and seal rings between rings and cooling line. This will probably impair the concentricity. The intensive machining causes high investment costs, but the operating costs will be reduced, due to the efficient heat transfer. This will also reduce the required cooling time. Figure 5.3 visualizes the concept of this design solution.

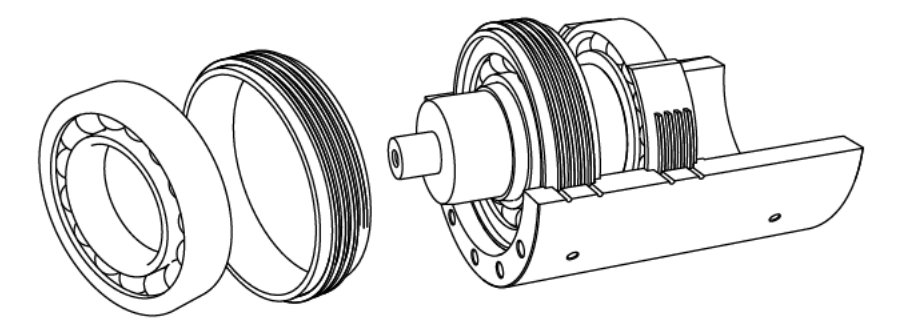


Figure 5.3: Cooling ducts inside the bearing seat

The cooling ducts are integrated in the housing and with the use of quick couplings, the cooling hoses can be easily detached. With detached cooling hoses, the mobility of the housing will hardly be restricted, which allows as convenient bearing exchange. Due to the integration of

the cooling ducts in the housing, the risk of leakage is rated as low.

Temperature system: 3

Investment costs: Acceptable

Operating costs: Good

Inconvenience of bearing exchange: Ideal Estimated space requirements: Sufficient

Hazard: Good Flexibility: Good

Cooling performance: Ideal
Automation capability: Ideal

5.2.2 Cooling tube in a groove on the outside of the housing

Intensive machining of the housing can be avoided, when the cooling line lays in a groove at the outside of the housing. But this also implies an enlargement of the distance between cooling duct and bearing. For the machining, the stands must be removed. But they are screwed to the housing, so this will not be critical. But that the stands are directly under the first groove position is not optimal. After the machining it would be useful to relocate the stands, so they are not in the area of the grooves. The cooling duct can be wrapped around the groove and be connected to T-piece adapters. An insulation layer can be applied at the outside of the cooling duct, to reduce cold loss. It must be considered, that the depth of the groove will effect the stiffness of the housing at the bearing position. A deeper groove will increase the cooling efficiency, but weakens the stiffness. The less intense machining will reduce the investment costs, but the increased distance to the bearing will probably increase the power consumption. The cooling ducts at the outside require a more careful handling of the housing. This will decrease the mobility and increase the risk of leakage. That they are outside of the housing will also increase cold losses to the environment, which will decrease the cooling performance.

Temperature system: 4 Investment cost: Sufficient Operating costs: Sufficient

Inconvenience of bearing exchange: Good **Estimated space requirements:** Sufficient

Hazard: Sufficient **Flexibility:** Good

Cooling performance: Good Automation capability: Ideal

5.2.3 Heat sink between the bearings

A heat sink between the bearings will not effect the contact area or the stiffness around the bearing position. The heat sink can be a ring made of a high thermal conductive metal, which has cooling ducts inside. The heat sink must be locked at axial and radial position, and the inner diameter must be greater than the shaft. As the heat sink must not move, it is not allowed to touch the bearing or the shaft. The connection to the cooling unit must lead through the housing, but there are only two holes necessary instead of four. A feather key connection with a specific groove length holds the heat sink in place, but also creates an area, where the outer ring of the first bearing is not in contact with the housing. A radial setscrew is a better alternative as the contact area of the bearings is not changed and there is no expensive machining at the housing necessary, but it will be difficult to rotate the heat sink in the right position after shoving the shaft inside the housing. The heat sink must be placed on the shaft before the last bearing is fitted. This means an additional assembly step for the bearing exchange is needed. The heat sink between the bearings will create an axial temperature distribution, one side of the bearing is colder than the other side. This is not a realistic condition, hence the cold air around turbines will cool the bearing circumferential. Certainly an advantage is that the heat sink in the middle reduces the air inside the test rig which also reduces the absolute humidity and therefore the icing. The connection holes in the housing are a difficult challenge, as the place for any couplings between the bearings is limited. The cross section of the cooling hose has to be reduced before entering the housing.

The manufacturing of the heat sink increases the investment costs, but the required changes to the housing stay low. Low operating costs are estimated, as the heat transfer is efficient. But the complicated assembly between the bearings increase the inconvenience. The risk of leakage during the bearing exchange is low, as the heat sink is inside.

Temperature system: 5
Investment cost: Acceptable

Operating costs: Good

Inconvenience of bearing exchange: Unsatisfying

Estimated space requirements: Sufficient

Hazard: Good Flexibility: Good Cooling performance: Ideal
Automation capability: Ideal

5.2.4 Axial cooling holes inside the housing

Holes in the housing in axial direction between the screw holes enable a constant circumferential temperature distribution, but with a small temperature difference between the bearing positions. The incoming supply cooling hose must be split into various small hoses which lead into the holes. On the backside the small hoses must be joined into the return hose. Hence the front panel must be disassembled regularly, quick couplings for the small hoses are useful. Inside the housing there is no need for hoses, the refrigerant can flow through the raw holes. To avoid leakage during disassembling, the quick couplings must be mounted on the housing, but not on the front panel. Therefore the front panel must be machined in a way that there is enough space for the couplings. The space between every hole of the front panel could be cut out, but this modification will decrease its stiffness. It is not possible to place the splitting unit in a central position, because of the shaft. If the splitting unit is in front of the front panel, the unit itself or one of the small hoses will probably rub against the rotating shaft. To avoid this, the small conduits can be lead around the corner of the front panel, so they end on the circumference of the housing. They can be fixed with a ribbon or 3d-printed clamps which are glued on the housing surface. For a constant circumferential temperature distribution it is important that all the small hoses after the splitting unit have the same length. On the back side a central placement of the splitting unit is not a problem, as there is no shaft in the middle. The quick couplings can be mounted directly on the back panel, because it does not have to get disassembled for the bearing exchange. But some kind of seal between housing and back panel might be necessary to avoid leakage.

The investment costs are slightly increased, because of the necessary machining. The small cooling hoses may need to be replaced once in a while, because the disassembly of the front panel may produce wear. The small hoses complicates the bearing exchange, as they have to be detached and attached for every exchange. This also increases the risk of leakage.

Temperature system: 6
Investment cost: sufficient
Operating costs: sufficient

Inconvenience of bearing exchange: Unsatisfying

Estimated space requirements: Sufficient

Hazard: Sufficient

Flexibility: Good

Cooling performance: Ideal
Automation capability: Ideal

5.2.5 Cooling coil around the housing

Instead of designing cooling ducts preferably near to the bearings, a copper tube can be wrapped around the housing, forming a cooling coil. This increases the distance to the bearing a lot, which will increase the operating costs and the required cooling time, but there is no extensive machining required, because the housing does not need intensive changes. The copper tube can also be used for other experiments. This method has been used for the rented cooling unit. Achieving equal temperatures at both bearings is complicated by space limitations. The front stand must be relocated to give access to the housing at the first bearing position. The cross section of a tube is circular. If the tube is wrapped around the housing like a coil, small air gaps will remain, which will have an adverse effect on the heat transfer. Gapfillers work best when they are pressed between the surfaces, but with their low compression rate they are not practical for this uneven gap. The small piece of gapfiller which separates the copper tube from the housing where they actually should be in contact, will probably decrease the thermal conductivity more than it can be increased by reducing the air gaps. Alternatives are heat pastes or thermal conductive adhesives. They will adapt to the shape of the tube much better, which results in a better heat transfer. But they often consist of hazardous material, which aggravates the application, the handling afterwards, and the disassembly. The cooling coil is on the outside of the housing and needs a proper insulation. Not only to reduce cold losses, but also to reduce icing.

Temperature system: 7
Investment cost: Good
Operating costs: Acceptable

Inconvenience of bearing exchange: Acceptable

Estimated space requirements: Sufficient

Hazard: Acceptable **Flexibility:** Ideal

Cooling performance: Acceptable
Automation capability: Ideal

5.2.6 Thermal fluid bath

Contact difficulties between housing and thermal fluid can be avoided, if the housing is surrounded by the thermal fluid. This can be achieved by two different ways: the housing is surrounded by a tight box, which is flooded with thermal fluid. The box includes only the housing, so the volume of thermal fluid is reduced and the torque meter and the drive can still operate at room temperature. The box must by well insulated, and the opening of the box for the coupling must be well sealed. The seal must not produce much friction, but must withstand the temperature difference and must keep the thermal fluid inside. If so much friction is produced, that the torque meter data cannot be used to make statements of the bearing, the torque meter should be placed inside. When the box is closed, it is flooded with thermal fluid. Flooding should be carried out by a pump system with an additional thermal fluid tank. When the thermal fluid fills the box and flows inside the cooling hoses to the cooling unit, the cooling unit can start the circulation of the thermal fluid. The inlet and outlet of the cooling hoses to the unit should be placed on opposite sides, to provoke a flow around the housing. The thermal fluid must be pumped down before every bearing exchange. An alternative is to lower the complete test rig into a pool of thermal fluid by a crane, but this requires a crane operator for every bearing exchange. The drive and also the torque meter must be replaced to withdraw the cold temperatures and the surrounded fluid. The pool must be well insulated, but the sealing is simpler than at the first option, because no rotating parts must be sealed. For every bearing exchange, the test rig must be lifted of the pool by a crane. It is useful to remove all cables, so the test rig can easily be moved to free space for the disassembling.

Both options have the advantage, that the heat transfer from thermal fluid to housing is very efficient. But as the thermal fluid is in direct contact with the housing, some kind of filter must be installed, to protect the pump from particles. The filter and thermal fluid replacements increase the operation costs. Leakages are also more critical. To keep the thermal fluid outside of the housing is also a challenge. The blend of components inside the grease influences the wear behavior a lot. Therefore it is very important, that no other component is added to the grease during the test. To keep the thermal fluid out of the housing, it must be sealed. At first, open and not used holes must be closed. That can be achieved by welding them shut, or to close them with fitting parts or bolts combined with isolating material like teflon or hemp tape, or screw glue. The sensor places must be sealed, too. The junction between housing and front panel can be sealed with a flat seal. This allows disassembly but must be renewed after a couple of bearing exchanges. The front panel has already a seal installed, which seals the housing to the shaft. But common seals are designed to keep fluids inside, and dust and

other particles outside. In this application, there is also fluid outside which will create a higher pressure on the seal than the closed air inside. A change of the seal model could be necessary.

Temperature system: 8
Investment cost: Acceptable

Operating costs: Good

Inconvenience of bearing exchange: Unsatisfying

Estimated space requirements: Acceptable

Hazard: Unsatisfying **Flexibility:** Good

Cooling performance: Ideal
Automation capability: Ideal

5.3 Peltier elements

As the efficiency of Peltier elements decreases with increasing cooling capacity, it is beneficial to use multiple elements in parallel. The required cooling capacity can then be distributed over multiple elements. The elements can be mounted on the housing, ideally around the bearing position. They can be mounted with thermal conductive adhesive directly on the housing or on a copper sheet which can be bent around the housing. A direct connection will benefit the conductivity, but a bend copper sheet will guarantee a better circumferential distribution and it enables a less complicated disassembly. The copper sheet can be contracted by a screw like in clamps. Similar to the cooling hose, the size of the elements must fit between the sheets of the stands, or the stands must be placed at another position. The Peltier elements must be wired in parallel. The cable must be connected to a current supply, where the current is controlled by the control software of the test rig. The cables will impede the bearing exchange and it has to be guaranteed, that the cables do not get damaged, while moving the housing. As the cooling capacity of single Peltier elements probably will not suffice, elements must be stacked on each other. To maximize the cooling capacity, which is necessary to reach low temperatures, the hot side of the Peltier elements must also be cooled. The heat losses are emitted exactly at their position, which will disallow an efficient use. Peltier elements work best, when the temperature difference between the two sides are as small as possible. This means, that the heat loss at the hot side has to be transported away. This process requires an additional cooling system, which makes the use of Peltier elements impractical in this case. Hence, Peltier elements are not respected in the following rating.

5.4 Considerations which apply to all concepts

Temperature changes influence the materials. Solid bodies expand with rising temperature, and shrink at sinking temperature. As the temperature is not homogeneously distributed and the thermal expansion coefficients vary between the different materials, components will not shrink simultaneously. This will cause changes in junctions and contact pressure. If the outer ring cools down faster than the inner ring, the contact pressure inside the bearing will increase, and therefore the friction torque will also increase. The influence of thermal expansion was noticed especially on the hydraulic cylinder. In order to fully exploit the automation possibilities of a temperature system, an automated regulation of the axial load is necessary.

The temperature not only influences the dimensions of components, but also physical properties. The electric conductivity of materials depends on temperature. As sensors measure their measurement parameters by the change of resistance, the measurement results might be distorted.

5.5 Final rating

For the subsequent comparison of the systems according to the VDI standard 2225 [65], the criteria are weighted by the author. The weight of the criteria are listed in Table 5.1.

Table 5.1: Conversion and weight of the criteria

Criteria	Weight
Estimated investment costs	5 %
Estimated operating costs	10 %
Inconvenience of bearing exchange	25 %
Estimated space requirements	10 %
Hazard	10 %
Flexibility	15 %
Cooling performance	20 %
Automation capability	5 %

The VDI standard 2225 [65] stipulates that the rating of ideal to unsatisfying is converted to a numerical scoring system from 0 (unsatisfying) to 4 (ideal). This requires an additional step, where the quality rating normalizes the results between 0 and 1. The step can be avoided by scoring the rating directly between 0 and 1, respectively 0 to 100 %. The scoring according to the VDI standard 2225 [65] and the direct normalized scoring is listed in Table 5.2.

Table 5.2: Scoring of the rating

	U	_		
Rating	Scoring	Scoring		
	VDI 2225	normalized		
Ideal	4	100 %		
Good	3	75 %		
Sufficient	2	50 %		
Acceptable	1	25 %		
Unsatisfying	0	0 %		

The rating of each system is now listed in Table 5.3. The total score S_i is calculated by the sum of the product of the individual criteria score $s_{i,j}$ and the weight w_j , where i is the index for the temperature system and j the index for the criteria (Equation 5.15).

$$S_i = \sum s_{i,j} \cdot w_j \tag{5.15}$$

Table 5.3: Rating of the temperature systems

		Temperature Systems							
Criteria	Weight	1	2	3	4	5	6	7	8
Estimated investment costs [%]	5	100	25	25	50	25	50	75	25
Estimated operating costs [%]	10	0	100	75	50	75	50	25	75
Inconvenience of bearing exchange [%]	25	0	75	100	75	0	0	25	0
Estimated space requirements [%]	10	100	25	50	50	50	50	50	25
Hazard [%]	10	100	100	75	50	75	50	25	0
Flexibility [%]	15	0	25	75	75	75	75	100	75
Cooling performance [%]	20	75	50	100	75	100	100	25	100
Automation capability [%]	5	0	100	100	100	100	100	100	100
Total [%]	100	40	61	83	68	58	54	45	48

Temperature system 3, a cooling unit with cooling ducts inside the bearing seat, has the best total rating. With over 80 % it is rated as very good according to the VDI standard 2225 [65]. This temperature system is recommended for the BEAT0.2 test rig in perspective of the author. The institute may use a different weighting of the criteria, which could lead to another temperature system recommendation.

6 Insulation design

In this chapter, the requirements for insulation are described and an insulation design is created by using the Morphological Box method.

6.1 Insulation specifications

The insulation must reduce the heat flow from the environment to the test rig as far as it is lower than the heat flow from test rig to the thermal fluid. The tests in Section 4 have also shown, that a simple insulation with insulation matts is insufficient to prevent icing. A solution is necessary to limit the access of air and humidity to the housing. Also the insulation must not restrict the handling of the bearing exchange in a critical way. The first two arguments form the purposes for the design:

- Reduction of heat flow from the environment
- · Limitation of icing

The final solution must fulfill the third argument:

• Low restriction during the bearing exchange

6.2 Manifestations of the parameters

The reduction of heat flow from the environment can be achieved by the insulation of the housing surface. Several materials and shapes are possible, a collection of them is listed as a morphological box in Table 6.1.

Table 6.1: Morphological box for the choice of insulation

Parameter		Characteristics					
Shape	Mats	Bag	Shaped blocks				
Material	Textile	Rubber	EPS	XPS	Aerogel		

Insulation mats can be applied to the housing. The insulation matter are available in various thicknesses and materials. They can be machine-cut to the right geometry, which will increase the durability and simplifies the application to the housing. Hook and loop fastener can be applied to the matters, to simplify the covering. An alternative is an insulation bag of two halves. The adaption to the housing will be complicated, but this ensures that the insulation fits well. A third option are to geometry of the housing shaped blocks. They can be stuck around the housing. It is not flexible, but will not wear out as fast as the matters.

Aerogel mats may be the most efficient insulation from thermal perspective. However, rubber mats adapt better to the surface. Textile insulation is the most ecofriendly solution, and as bag insulation it would provide a convenient access to upper halve of the housing. However, the friction between plate and bag would restrict the mobility of the housing and would lead to wear at the bag. Shaped blocks made of XPS can easily be removed to gain access to the screws of the feet of the housing. That is why this solution is preferred. In addition, it is recommended to place a plate of insulating material between housing and aluminum plate to reduce the cold losses over the feet of the test rig. For the low temperature tests in Section 4 a wood plate and a Plexiglas pane were used. A wood plate is a cheap and good insulator, but for future tests a transparent material is preferred, to allow a view of the groove stones. A Plexiglas pane is recommended, because it is also not vulnerable against humidity.

It is unlikely, that the insulation sits tight enough on the housing, that no air from the outside has access to the housing surface, where it can condensate and freeze. Hence, the humidity of the air must be reduced, or the amount of air with possible contact to the housing surface. To reduce the humidity, dehumidifier could be installed in the room, where the test rig is placed. But as the room is often used as a passage, and the doors are often open for ventilation, the air is frequently replaced. This does not allow an efficient use of dehumidifiers. A simpler way is to limit the amount of air with direct contact to the housing. The air can be kept away by putting the test rig inside an air tight box. The box does not need to fulfill any thermal insulation purposes, but an isolation purpose. The design parameters are listed as a morphological box in Table 6.2.

The handling of the box partly depends on the dimension. It could include the whole test rig, or just components of it. The drive requires cooling by air convection, and for mass reduction, the box should be designed as lightweight as possible. So it is useful to exclude the drive, but to use the shape of the drive stand as support. This also means that no rotating parts need

Table 6.2: Morphological box for the choice of isolation

Parameter	Characteristics					
Dimension	Only	Housing to	Housing	Complete		
of the box	of the box housing torque meter		to drive	test rig		
Opening	Hatch	Cover				
Material of	Wood	Plexiglas and	EPS			
the box		aluminum profile				
Material of	Rubber	Vacuum	EPS	Aerogel		
box insulation		panels				
Air displacement Nitrogen		Dry air	Padding	None		
substance			material			

to be sealed. A hatch has the advantage, that the box does not need to be placed somewhere else while removing the shaft and the bearings. But the mobility is limited due to the right side of the box. The hatch can be designed so that half the box can be folded upwards, but the curved part of the drive stand complicates the sealing at the opening. A cover instead could be lifted and does not limit the mobility. If all cables and hoses go through the plate, now openings have to be installed into the cover. Wood as the material for the box would be a cheap and ecofriendly solution, but it is not lightweight and humidity could effect the edge contour over time which would worsen the sealing. Styrofoam is light, but also breaks quickly. The combination of Plexiglas and aluminum profiles is a expensive but also durable option. For the left side at the drive stand only a Plexiglas pane is usable, because the profile can not be adapted to the drive stand. Some kind of sealing compound should be added at the transition of Plexiglas pane to aluminum profile, to reinforce the sealing. The transparency is also helpful at institute tours for potential industrial partners, as the test rig is visible during the test run. If it is noticed, that the insulation is not sufficient, additional insulation can be added to the box on the inside. The rectangular and even shape of the box allows the use of vaccum panels, which has great insulation properties, but they are also expensive. The simplest insulation would be a layer of rubber insulation. Of course, this would remove the transparency.

Another optional addition is the usage of air displacement substances. This would remove a large portion of the air volume and the including water vapor. But also without air displacement substances, no critical icing is expected. Absolute humidity is measured grams of water per kilogram wet air. Mollier's h-x diagram [11] allows the graphical determination of the absolute humidity, which is measured in grams of water vapor per kilogram dry air. At a room temperature of 27 °C and a relative humidity of around 65 %, the absolute humidity is

around 15 g/kg. Assuming the box's volume at around 0.25 m³, where half of the volume is already occupied by the test rig and its insulation, and an air density of around 1 kg/m³, leads to the estimation that there are around 125 g dry air and less than 2 g water vapor inside the box. The icing of this low amount of water vapor will not have a critical effect on the cooling performance, but the amount can be further reduced, by flushing the box with nitrogen or dry air or filling the box with padding material. A slightly over pressure will also prevent the air outside to come inside. An evacuation is also possible. The air pressure outside will press the box on the plate and increases the sealing.

To ensure a tight seal, the bottom of the cover must be equipped with a seal. Draw latches can be used to press the box on the plate. Holes in the cover for the cooling hoses and cables can be avoided by leading them through the plate.

6.3 Conclusion of the chosen characteristics

As insulation, shaped blocks made of XPS are preferred. A Plexiglas pane is placed between the test rig and the aluminum plate. An isolation box is used to limit the icing. The box includes the housing and the torque meter and uses the stand of the drive as a support. The box is made out of Plexiglas and aluminum profiles which guarantees a long durability and enables a view on the test rig during a test run. A seal is applied under the bottom box edge and the box is pressed by draw latches on the plate. If the insulation is not sufficient, the box can be applied with a layer of rubber insulation from the inside. An air displacement substance should not be necessary. Figure 6.1 shows the conceptional design of the insulation.

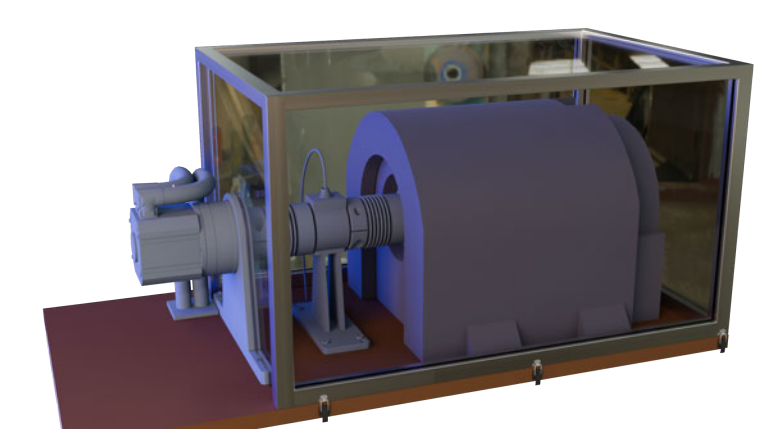


Figure 6.1: Conceptional design of the insulation, without cooling hoses

7 Thermal model

To find a suitable cooling unit, the required supply temperature and the cooling capacity at this temperature has to be determined. The tests with the rented cooling unit in Section 4 give a useful recommendation for the BEAT0.2 test rig, but also opens the opportunity to build and validate a thermal model, which can be used to determine cooling unit specifications for future cooling projects. The thermal model bases on the fundamental equations of heat transfer theory and simplified geometry of the modified test rig using MATLAB Simulink (version R2023b). The following sections describe the structure of the model and assumed simplifications. The final MATLAB and Simulink files can be found on the CD enclosed with this document. The simulation can be started with the execution of "runThermalModel.m".

7.1 Basic structure of the model

The dependence of temperature and heat energy enables an approximate prediction of the temperature behavior of the test rig by calculating the heat flows between the components and the environment. For the calculation of the current temperature, Equation 2.6 from Section 2.1 is used. The implementation in a Simulink subsystem is shown in Figure 7.1.

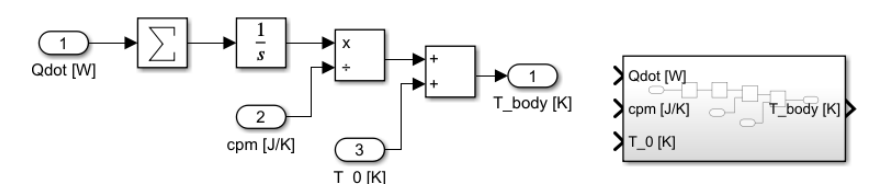


Figure 7.1: calculation of the temperature (left) and the final subsystem (right)

Qdot is the collection of incoming and outcoming heat flows \dot{Q} . cpm is the product of the specific heat capacity c_p and the mass of the current component m. T_0 is the initial temperature of the component. The calculation of the heat flow is performed with Equation 2.12 from Section 2.2. The implementation is shown in Figure 7.2.

T_contact is the temperature of the adjacent component, G is the conductance between the

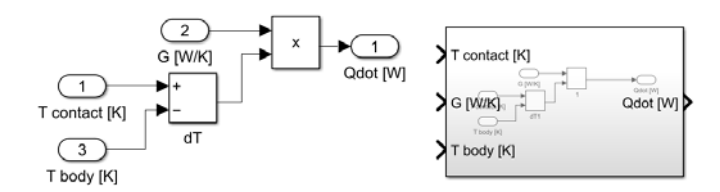


Figure 7.2: Calculation of a heat flow (left) and the final subsystem (right)

current component and the adjacent component, and T_body is the temperature of the current component. Each component of the test rig is represented with the subsystem in Figure 7.1 and connected by their current temperatures.

7.2 Geometrical and thermal simplification of the test rig

Due to the radial symmetrical form of the test rig, its geometry will be fragmented in tubes and rings to simplify the calculation, which is visualized in Figure 7.3.

Following assumptions are also used: Thermal contact conductance is neglected, as it requires more information about the component's surface and pressure between the components. This would increase the complexity of the model. Only constant values for heat capacity and thermal conductance are used. In reality they depend on temperature. Thermal expansion is also neglected. Only heat conductance is used. Heat convection and radiation will be neglected. The temperature of the environment will be assumed as constant. Holes and screws will be ignored. The system borders are the surface of the housing with an additional 20 mm layer of insulation, the coupling between torque meter and shaft and the feet of the housing. The used material properties are listed in Table 7.1. Heat flows are only calculated in two dimensions: axial and radial direction. In axial direction, they are calculated between each center of mass with Equation 7.16, which is formulated for a heat flow through a wall. In radial direction the heat flow is calculated between the radii, where the material outside of the radius has the same mass as the material inside. This medium radius r_m is calculated with Equation 7.18. The heat flow itself is calculated with Equation 7.17, which is formulated for a heat flow between the inside and outside of a tube. The material between those target points is assumed as insulation with its thickness s_i , its thermal conductivity k_i , its width l for radial flows or its cross section A for axial flows.

$$\dot{Q}_{ab,axial} = \frac{1}{\sum \frac{s_i}{k_i}} \cdot A_{ab} \cdot \Delta T_{ab} \tag{7.16}$$

$$\dot{Q}_{ab,radial} = \frac{1}{\sum \frac{1}{k_i} \cdot ln(\frac{r_i}{r_{i+1}})} \cdot 2\pi \cdot l_{ab} \cdot \Delta T_{ab}$$
(7.17)

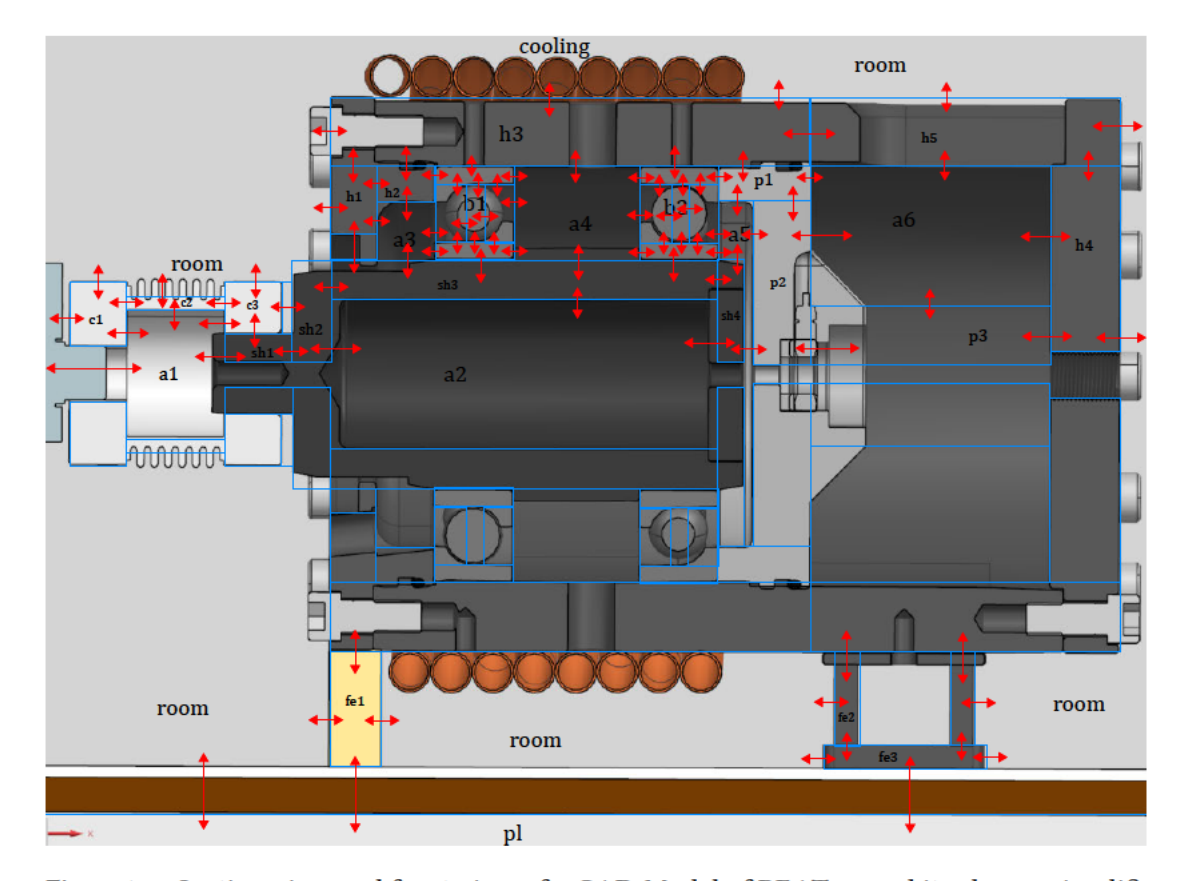


Figure 7.3: Section view and front view of a CAD Model of BEAT0.2 and its chosen simplifications. This view, the front view, and the back view are also on the CD enclosed with this document

$$r_m = \sqrt{\frac{r_{outer}^2 + r_{inner}^2}{2}} \tag{7.18}$$

Both equations can be separated in two parts. The first part is the temperature difference ΔT , which has the unit [K] and changes during the simulation. The second part has the unit [K] and is described as the conductance G. It depends on material properties and dimensions, which are assumed as constant. Therefore G will be precalculated in MATLAB.

For a better explanation, the calculation of the conductances of one component is shown below. As shown in Figure 7.4 the coupling is separated in 3 components: c1, c2, and c3. The focus of this exemplary calculation is on c3. This component is in heat exchange with a1, c2, sh1, sh2, and the air of the room. Each heat flow is visualized in Figure 7.4 with an arrow, the observed ones for c3 are red. Flows from small areas like from c3 to room, but axial over c2 are

Table 7.1: Material Properties

Property	Value	Unit	Description of index
$\overline{ ho_{al}}$	2800 [46]	$\frac{kg}{m^3}$	Aluminum
$ ho_{st}$	7800 [46]	$\frac{kg}{m^3}$	Steel
$ ho_a$	1.184 [6]	$\frac{kg}{m^3}$	Air
$ ho_{stst}$	8000 [46]	$\frac{kg}{m^3}$	Stainless steel
$ ho_{wood}$	600 [44]	$\frac{kg}{m^3}$	Wood
$ ho_l$	1000 [67]	$ \begin{array}{c c} m\\ \frac{kg}{m^3} \\ \frac{kg}{m^3} \end{array} $	Lubrication
$ ho_{oil}$	920 [49]	$\frac{kg}{m^3}$	Water
k_{al}	220 [47]	$\frac{W}{m K}$	Aluminum
k_{st}	46.5 [47]	$\frac{W}{m K}$	Steel
k_a	0.02 [48]	$\frac{W}{m K}$	Air (steady)
k_{seal}	0.16 [45]	$\frac{W}{m K}$	Seal around shaft
k_{ins}	0.033 [30]	$\frac{W}{m K}$	Insulation
k_{stst}	15 [49]	$\frac{W}{m K}$	Stainless steel
k_{plexi}	0.184 [45]	$\frac{W}{m K}$	Plexiglas
k_{wood}	0.2 [45]	$\frac{W}{m K}$	Wood
k_l	0.138 [67]	$\frac{W}{m K}$	Lubrication
k_{cu}	380 [47]	$\frac{W}{m K}$	Copper
$c_{p,oil}$	1550 [49]	$\frac{J}{kg K}$	Thermal oil
$c_{p,al}$	896 [46]	$\frac{J}{kg K}$	Aluminum
$c_{p,st}$	502 [46]	$\frac{J}{kg K}$	Steel
$c_{p,a}$	1000 [43]	$\frac{J}{kgK}$	Air
$c_{p,stst}$	477 [46]	$\frac{J}{kgK}$	Stainless steel
$c_{p,wood}$	1800 [44]	$\frac{J}{kgK}$	Wood
$c_{p,l}$	2103 [67]	$\frac{J}{kg K}$	Lubrication

neglected. To keep track of the different heat flows, following notation was considered: for axial heat flows the left component is mentioned first, for radial flows the bigger component. For the conductances of c3 this results in $G_{c2,c3}, G_{a1,c3}, G_{c3,sh1}, G_{c3,sh2}, G_{room,c3}$. The heat flow between c2 and c3 is in axial direction. It contains two layers: half of c2 (stainless steel) and half of c3 (aluminum). The dimensions are measured in the CAD-Model of the test rig in Siemens NX. The indices stand for r as the inner radius, R as the outer radius, x, y, z as the

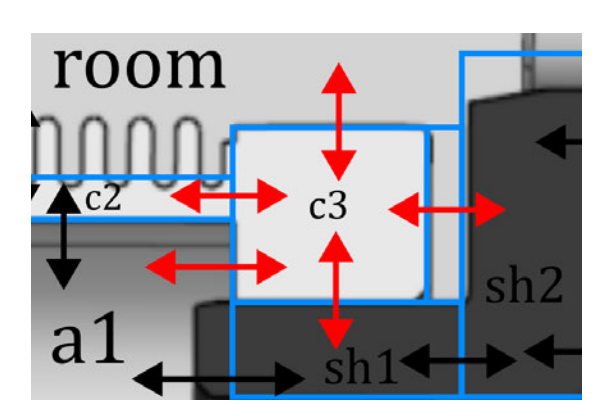


Figure 7.4: Heat flows of c3

dimension in each direction, s as the thickness in a nonspecified direction. The contact area $A_{c2,c3}$ is also needed and calculated in Equation 7.19.

$$A_{c2,c3} = \pi \cdot (c2_R^2 - c2_r^2) \tag{7.19}$$

The conductance between c2 and c3 is then calculated in Equation 7.20.

$$G_{c2,c3} = \frac{1}{\frac{c2_x}{2 \cdot k_{stst}} + \frac{c3_x}{2 \cdot k_{al}}} \cdot A_{c2,c3}$$
 (7.20)

 $G_{a1,c3}$ and $G_{c3,sh2}$ are calculated using the same method in Equation 7.19 to 7.20.

$$A_{a1,c3} = \pi \cdot (c2_r^2 - c3_r^2) \tag{7.21}$$

$$G_{a1,c3} = \frac{1}{\frac{a1_x}{2 \cdot k_a} + \frac{c3_x}{2 \cdot k_{cl}}} \cdot A_{a1,c3}$$
 (7.22)

$$A_{c3,sh2} = \pi \cdot (c3_R^2 - c3_r^2) \tag{7.23}$$

$$G_{c3,sh2} = \frac{1}{\frac{c3_x}{2 \cdot k_{al}} + \frac{sh1_x - c3_x}{k_{air}} + \frac{sh2_x}{2 \cdot k_{st}}} \cdot A_{c3,sh2}$$
 (7.24)

For the calculation of $G_{room,c3}$ and $G_{c3,sh1}$ Equation 7.17 is used in Equation 7.26 and 7.27. The radii are calculated with Equation 7.18. To every area which is in contact with the room, a layer of insulation s_{ins} is added.

$$c3_{mr} = \sqrt{\frac{c3_R^2 + c3_r^2}{2}} \tag{7.25}$$

$$G_{room,c3} = \frac{2\pi \cdot c3_x}{\frac{1}{k_{ins}} \cdot ln(\frac{c3_R + s_{ins}}{c3_R}) + \frac{1}{k_{al}} \cdot ln(\frac{c3_R}{c3_{mr}})}$$
(7.26)

$$G_{c3,sh1} = \frac{2\pi \cdot c3_x}{\frac{1}{k_{al}} \cdot ln(\frac{c3_{mr}}{c3_r}) + \frac{1}{k_{st}} \cdot ln(\frac{sh1_R}{sh1_r})}$$
(7.27)

These conductances are then added as constants to a Simulink subsystem which represents this component (Figure 7.5). Each heat flow has its heat transfer subsystem which is connected to the conductance, the component temperature, and the contact temperature. The resulting heat flows are collected and connected to the component temperature subsystem.

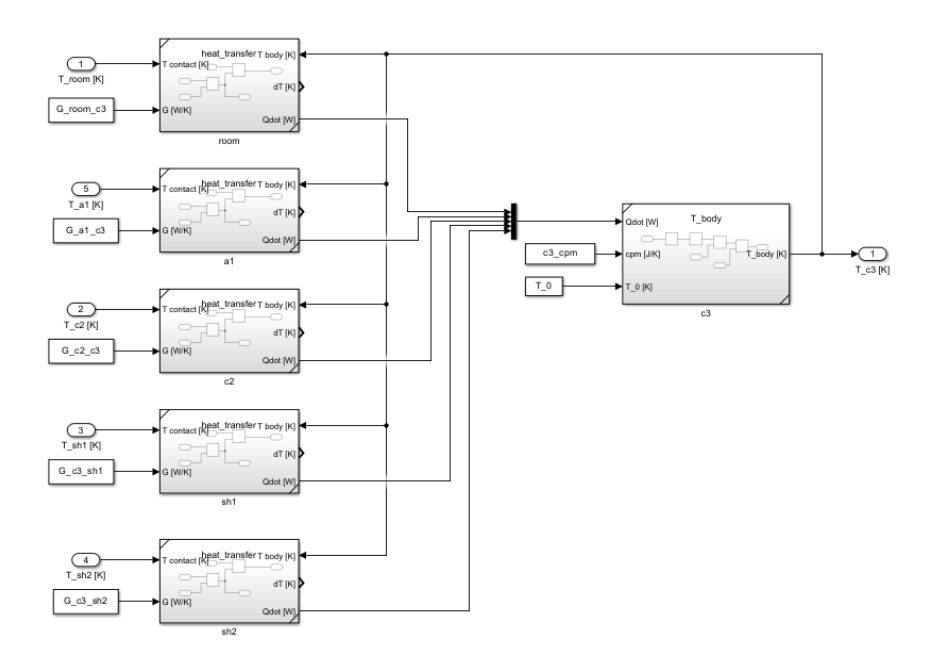


Figure 7.5: Simulink subsystem of component c3

7.3 Modelling of the bearing

The bearings were separated in tubes and rings too. The ramp on the race way of the outer ring (bo) was removed, but the inner diameter was changed, so the mass stays equal to the mass of the real bearing. The same changes were applied to the inner ring (bi), but with the outer diameter. The 15 rolling elements n_{re} were replaced by a single ring (bb). The thickness of the ring bb_x was calculated in a way, that the mass of the ring equals to the total mass of the rolling elements 7.28. The lubrication (l) was replaced by two rings left and right from the rolling elements ring. Both lubrication sides will be seen as a combined component, because in

reality the lubrication goes through the gaps between the rolling elements. A visualization of the simplification including the heat flows is shown in Figure 7.6.

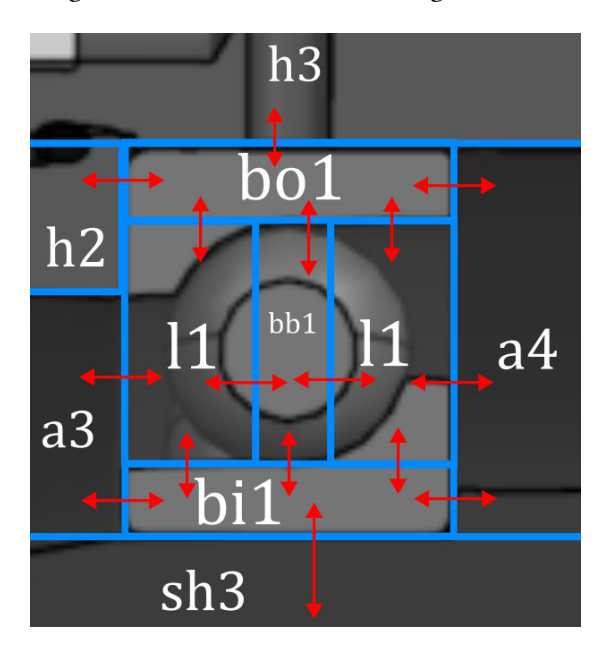


Figure 7.6: Simplification of the bearing at first bearing position

$$bb_x = \frac{4}{3} \cdot \frac{n_{re} \cdot r_{re}^3}{bo_r^2 - bi_R^2} \tag{7.28}$$

7.4 Connection of test rig and cooling unit

Cooling unit

The cooling capacity of the cooling unit is limited and depends on temperature among others. The temperature dependency is given by the manufacturer and listed in Table 4.2. To implement the dependency of temperature into the model, a mathematical function is needed. The values of Table 4.2 are plotted as crosses in Figure 7.7 to guess the function type. The point set can be separated into a constant (for $T \geq 0$) and a curved part. By plotting the curved part and using the "Basic Fitting" tool from MATLAB the coefficients for a cubic function can be determined. A cubic function was chosen, because this type has the lowest deviation. The function is used for temperature values from $-50\,^{\circ}C$ to $0\,^{\circ}C$. Everything above is set to a constant cooling capacity value of $5.3\,kW$. The point set and the approximated function is plotted in Figure 7.7. This function does not describe how much heat can be extracted from the test rig, but from

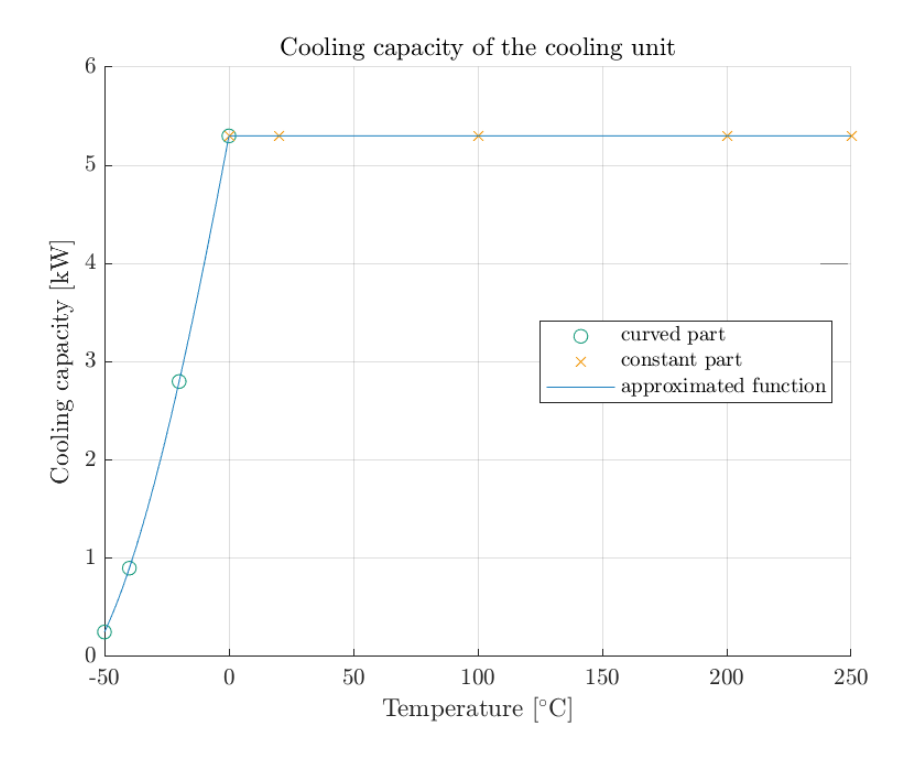


Figure 7.7: Cooling capacity of the cooling unit

the thermal fluid, in this case a thermal silica oil, which flows around the test rig. The cooling capacity effects the difference between return and supply temperature. The calculation of the temperature change differs to the previous calculations, because it is now dealt with a mass flow \dot{m} and not with a steady mass m. The mass flow is the product of volume flow rate \dot{V} and the density ρ . Only the maximum volume flow rate is known, but it is assumed that the volume flow rate is proportional to the pump speed. The current pump speed is part of the validation data. The factor f_{pump} is used for all proportional pump speed relations. The factor is calculated in Equation 7.29 and the mass flow in Equation 7.30.

$$f_{pump} = \frac{n_{pump}}{n_{pump,max}} \tag{7.29}$$

$$\dot{m}_{oil} = f_{pump} \cdot \dot{V}_{oil,max} \cdot \rho_{oil} \tag{7.30}$$

Together with the cooling capacity \dot{Q}_{unit} and the specific heat capacity of the oil $c_{p,oil}$ the temperature change is calculated in Equation 7.31.

$$\Delta T_{unit} = \frac{\dot{Q}_{unit}}{\dot{m}_{oil} \cdot c_{p,oil}} \tag{7.31}$$

 ΔT_{unit} must be subtracted from T_{return} to get the supply temperature T_{supply} (Equation 7.32).

$$T_{sumly} = T_{return} - \Delta T_{unit} \tag{7.32}$$

Of course the supply temperature is not allowed to come below the set value. This behavior can be achieved by the switch block in Simulink (second block from the right in Figure 7.8). The control input of the block decides, which input is forwarded. If the supply temperature is above the set value, the supply temperature is forwarded. If the supply temperature equals or is less than the set value, the set value is forwarded. The cooling capacity function and Equations 7.30 to 7.32 are combined in a Simulink subsystem (Figure 7.8). As T_{supply} and T_{return} must be known in the beginning, am initial condition is added by the unit delay (1/z) block. It sets the initial temperature to room temperature.

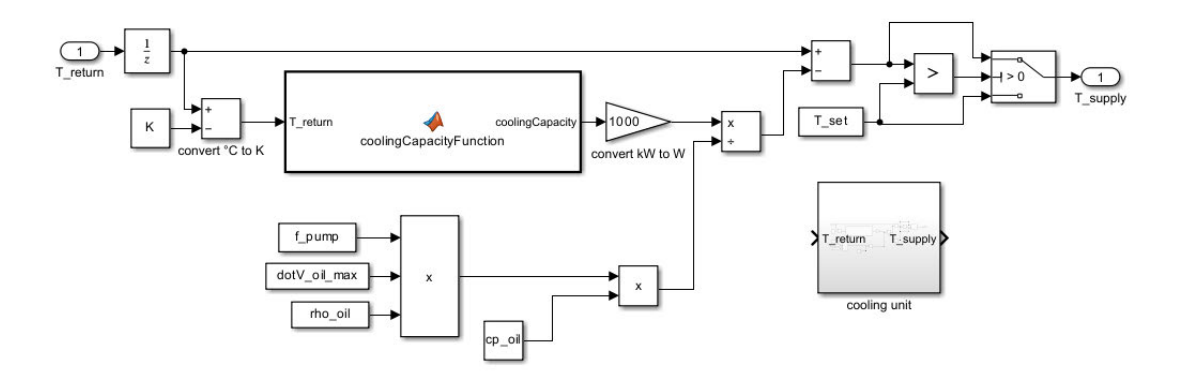


Figure 7.8: The cooling unit as a subsystem

Cooling hose

The supply temperature which is set on the cooling unit does not act directly on the test rig. The thermal fluid has to be transported through the supply hose. On the way it absorbs heat from the environment, which causes a temperature rise. Equation 7.33 describes the temperature change in a tube in axial direction [64]. It can be rearranged to the temperature at the end of the hose $T_{hose,end}$ with Equation 7.34.

$$T_{hose,start} = T_{room} - (T_{room} - T_{hose,end}) \cdot e^{-\varepsilon}$$
(7.33)

$$T_{hose,end} = (T_{hose,start} - T_{room}) \cdot e^{\varepsilon} + T_{room}$$
(7.34)

The emissivity can be calculated with Equation 7.35 [64].

$$\varepsilon = \frac{k_{hose} \cdot l_{hose}}{\dot{V}_{oil} \cdot \rho_{oil} \cdot c_{p,oil}} \tag{7.35}$$

As $k_{hose} \cdot l_{hose}$ has the same unit as conductance, Equation 7.17 is used to calculate the upper part (Equation 7.36). This change results in Equation 7.37.

$$G_{hose} = \frac{\pi \cdot l_{hose}}{\frac{1}{k_{iso}} \cdot ln(\frac{r_{hose} + s_{iso}}{r_{hose}})}$$
(7.36)

$$\varepsilon = \frac{G_{hose}}{\dot{V}_{oil} \cdot \rho_{oil} \cdot c_{p,oil}} \tag{7.37}$$

 ε is assumed as constant, so it is precalculated in MATLAB and added to a Simulink subsystem (Figure 7.9).

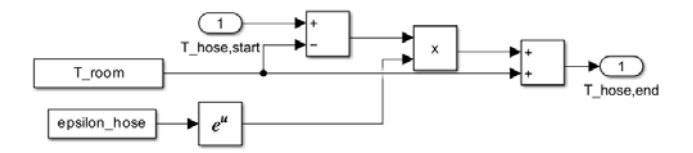


Figure 7.9: Hose subsystem in Simulink

Cooling coil

The oil flows from the hose into the cooling coil which is wrapped around the housing of the test rig. The cooling tube has a circular cross section. Therefore, the radial distance from housing to tube surface is not constant. The gap between tube and housing is filled with air. The more air there is between tube and housing surface, the lower is the conductance, because air has a lower conductivity than copper or steel. To include this effect into the model, the contact region of h3 and one half of the copper tube is split into infinitesimally small slices. The result is then multiplied 17 times, which equals the 8.5 rotations around the housing. The relation is shown in Figure 7.10. The height of the gap $s_{gap}(x)$ between housing and tube is calculated in Equation 7.38.

$$s_{gap}(x) = t_R - \sqrt{t_R^2 - x^2} (7.38)$$

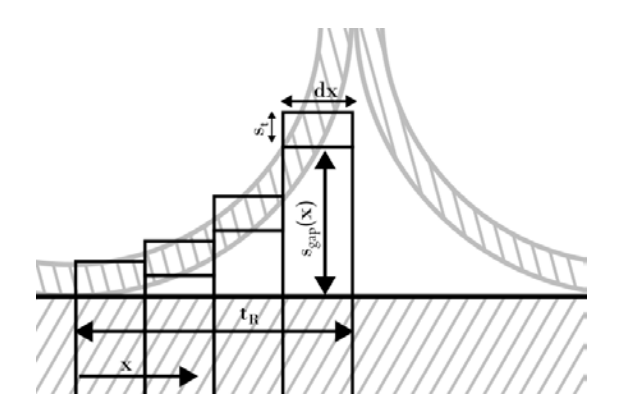


Figure 7.10: Discretization of the gap between cooling coil and housing

The on x depending distance and the thickness of the copper tube s_t are inserted into the calculation of the radial heat flow (Equation 7.39).

$$G_{coil,h3} = 17 \cdot \int_0^{t_R} \frac{\pi}{\frac{1}{k_s t} \cdot ln(\frac{h3_R}{h3_r m}) + \frac{1}{k_a} \cdot ln(\frac{h3_R + s_{gap}(x)}{h3_R}) + \frac{1}{k_c u} \cdot ln(\frac{h3_R + s_{gap}(x) + s_t}{h3_R + s_{gap}(x)})}} dx$$

$$(7.39)$$

The conductance between the room and the coil is calculated similar to Equation 7.39 but with the simplified contour of the coil $coil_R(x)$ (Equation 7.40). Instead of air, a layer of insulation is on top of the tube. The conductance is calculated in Equation 7.41.

$$coil_R(x) = h3_R + t_R + \sqrt{t_R^2 - x^2}$$
(7.40)

$$G_{room,coil} = 17 \cdot \int_0^{t_R} \frac{\pi}{\frac{1}{k_{cu}} \cdot ln(\frac{coil_R(x)}{coil_R(x) - s_t}) + \frac{1}{k_{iso}} \cdot ln(\frac{coil_R(x) + s_{iso}}{coil_R(x)})} dx$$
 (7.41)

The conductance $G_{coil,h3}$ is multiplied with the temperature difference between h3 and the medium temperature of the coil. The conductance $G_{room,coil}$ is multiplied with the temperature difference between room and coil. Both are summed and divided by the product of mass flow and heat capacity of the oil. Finally the supply temperature is added to the calculation (Equation 7.43). The medium temperature is calculated in Equation 7.42.

$$T_{coil} = \frac{T_{coil,supply} + T_{coil,return}}{2}$$
(7.42)

$$T_{coil,return} = \frac{G_{coil,h3} \cdot (T_{h3} - T_{coil})}{c_{p,oil} \cdot \dot{m}_{oil}} + T_{coil,supply}$$
(7.43)

The implementation in Simulink is shown in Figure 7.11. Again, a unit delay block is added, to set the initial temperature to room temperature. The final model and its connections are shown

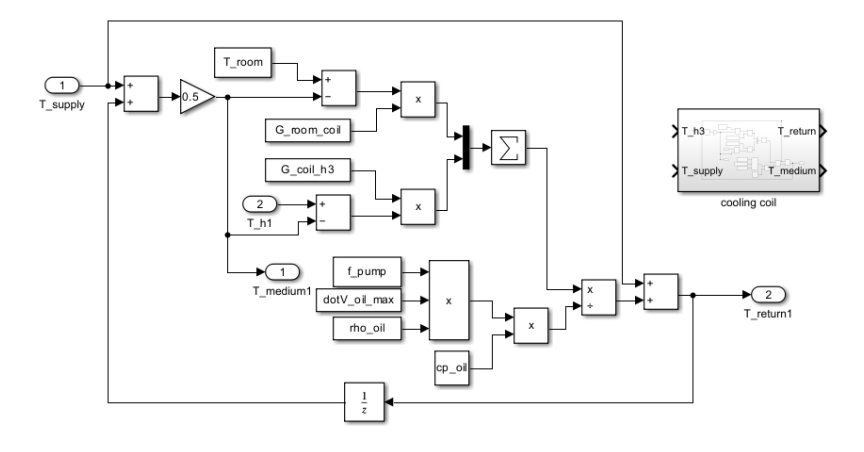


Figure 7.11: Cooling coil as a subsystem in Simulink

in Figure 7.12. Each block output can be observed now, for example the temperatures of the components, but also the heat flows. The temperature of the first outer ring of the bearing is fed into the Simulation stop system. This subsystem stops the simulation, when the temporal derivation is below $10^{-7}\frac{K}{s}$.

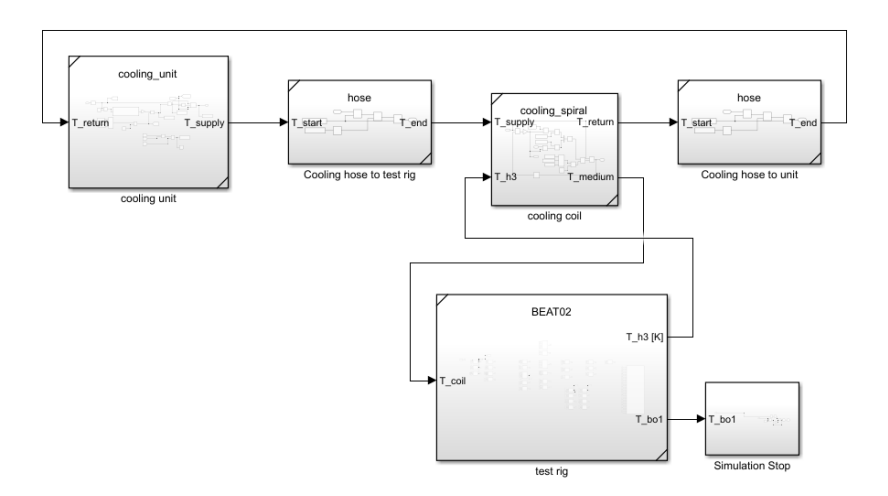


Figure 7.12: Thermal model in Simulink

7.5 Validation

While the rented cooling unit was at the institute, it was possible to get experimental data which can be used to validate the model.

7.5.1 Validation process

The original validation strategy was setting up a supply temperature, waiting until the process temperature does not change anymore and then notating the final temperature. This procedure should be repeated with different supply temperatures, but the same starting condition: every components temperature is at room temperature. As the cooling and also the heating process take a lot of time, and the time with access to the cooling unit was limited, the validation process was changed. To speed up the cooling process, instead of the supply temperature the process temperature was controlled. The reference temperatures were controlled one after the other, without heating the components back to room temperature. This temperature program ran almost for 45 hours, so it was not possible to manually adjust the temperatures. That is why it was tried to set the holding time long enough so that the temperature achieves a constant state. Figure 7.13 shows the temperature program including the bearing test at 0°C process temperature. After the test was finished, the process temperature was set to -20°C for five hours, then -40°C for ten hours. This temperature could not be achieved, because of the supply temperature limit of -50°C. Also the necessary holding time was underestimated, so the stagnation temperature was not achieved. After the ten hours, the process temperature was set to -30°C for four hours and then -10°C for four hours. Finally the supply temperature was controlled for a linear temperature rise. Because the necessary holding time for a stagnating

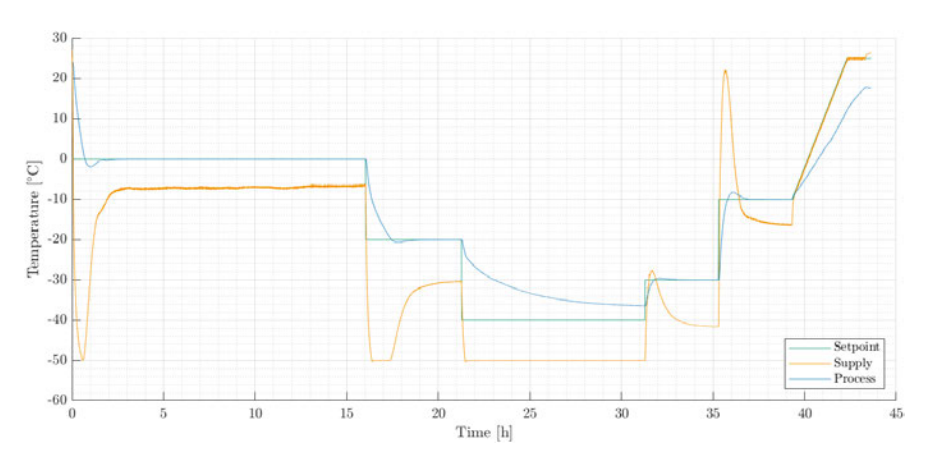


Figure 7.13: Temperature program for validation

temperature at -50°C supply temperature was not satisfied, the values of the process temperature were extrapolated. Also the supply temperatures of reference 2, 4 and 5 were extrapolated, because they did not stagnate either. The final temperatures are listed in Table 7.2.

 Reference
 T_{supply} in °C
 n_{pump} in rpm $T_{process}$ in °C

 1
 -9.03
 2999
 -0.05

 5
 -16.56
 2999
 -9.99

 2
 -30.25
 2999
 -20.00

-41.63

-50.00

2999

2999

-29.99

-36.88

Table 7.2: Experimental data for validation

It is noticeable, that the difference between supply and process temperature at reference 5 is less than the temperature difference at reference 1. It would be expected, that the difference of reference 5 is higher, because the process temperature is lower. Lower process temperature causes a higher heat flow from the environment, which would also make a higher heat flow to the coil necessary for compensation. To increase the heat flow, the supply temperature must also be increased. As the test rig was already cooled down to under -35 °C, the inner components were still colder than they would be if the validation process for this temperature started at room temperature. Colder components need a less low supply temperature.

7.5.2 Comparison between simulated and experimental data

4

3

This simulation uses an automatic selected solver with a fixed step size of 0.01 s. The stop time is set to 100 hours, but as already mentioned, the simulation will stop, if the temporal derivation of the temperature of the outer ring of the first bearing is below $10^{-7} \frac{K}{s}$. The room temperature is set to 27 °C. The model is simulated with the parameters of Table 7.2. The process temperature of the model is the temperature of the outer ring of the first bearing. The results are compared to the validation data in Table 7.3.

Reference T_{supply} in $^{\circ}C$ $T_{process}$ in $^{\circ}C$ Simulated $T_{process}$ in °C P_{unit} in W-9.03 -0.05 -2.63 40.05 1 5 -9.99 -16.56 -8.83 48.42 2 -30.25 -20.00 -20.08 63.63 4 -29.99 -41.63 -29.4476.28 3 -50.00 -36.88 -36.33 85.58

Table 7.3: Experimental and simulated data

To quantify the precision of the simulation, the root mean square error RMSE is calculated in Equation 7.44 [40].

$$RMSE = \sqrt{\frac{\sum (T_{process,exp,i} - T_{process,sim,i})^2}{n_{reference}}} = 1.31K$$
 (7.44)

With a *RMSE* of 1.31 K the prediction of the temperature is close to the experimental data. This is unexpected, as the insulation in the experiment should have more imperfections than the insulation in the simulation. But some assumptions could compensate the perfect insulation. In the simulation, the air of the room has a constant temperature and convection is ignored. In reality the air near by the housing cools down, too. This causes a lower temperature difference to the housing and with that a lower heat flow. Convection induces a replacement of air around the housing and the heat is led away, but this does not happen instantly and it does not prevent a temperature fall off near by the housing. Because of the large volume of air inside the room and the heat losses from the unit, the cold air does not have a relevant effect on the average air temperature. In addition some of the areas of the test rig are counted twice. For example the area between the feet and the housing is also counted in the contact area to the room. Additional experimental data in form of temperature at different locations of the test rig would help to evaluate the reliability of the model.

The model can also give information about the cooling time and the required cooling capacity for this temperature and insulation conditions. But both values can not be validated. The rented unit was not able to log the cooling capacity. Also the temperature regulation differs to the model. The unit was programmed to reach the desired process temperature as fast as possible. That is why the supply temperature at the beginning falls way below the stagnating supply temperature (noticeable in Figure 7.13 between 15 h and 20 h on the time-axis). The supply temperature of the model starts at room temperature and decreases according to the cooling capacity curve (Figure 7.7), but never is below the desired supply temperature. It was tried to simulate the controller behaviour of the unit, by integrating a PID-Controller with the controller values of the unit into the model. This would allow a better comparison of the cooling time, but the results were not satisfying, as the behaviour of the simulated controller differed a lot to the actual controller. An evidence for an in general much shorter cooling time of the model can give Figure 7.13 at the third reference with a supply temperature of -50°C. The figure shows that 10 hours was not enough time for the cooling process to cool down the bearing from -20°C to a stagnating temperature of -36.88°C. The model reached the stagnating temperature of -35.82 °C already after around 8 hours with a final temporal

temperature derivation of less than $10^{-7} \frac{K}{s}$, but the model started at room temperature and not at -20°C. A reason for the shorter cooling time could be, that condensation and icing were not respected. At room temperature the water is in its gaseous phase inside the air. With decreasing temperature, the water vapor condensates and accumulates as water drops at cold surfaces. The water freezes when the temperature is below 0°C. These two phase changes, from vapor to water (condensation) and from water to ice (solidification), release heat, which has to get compensated by the cooling unit. This compensation takes time.

8 Conclusion

The work carried out for this thesis encompassed the conceptual design of a temperature system for a bearing test rig. The thesis introduced modern cooling methods and insulation materials. Most notable results of preliminary tests with a temporary cooling unit are the significant influence of any gaps in the insulation on ice formation on the test rig structure and the exceedance of the allowable drive torque at -20°C process temperature. Test runs with 4 different greases at 0°C and -10°C were made and compared with test results of test runs at room temperature. The results showed an increase of friction torque at low temperatures in almost every test. The test procedure duration was increased by 25 minutes for insulation detaching and attaching, 1.5 hours for cooling to 0°C, respectively 3.5 hours for -10°C and additional 2 hours for defrosting. A second person was also needed for 10 minutes of work. It was possible to cool down the test rig to a bearing temperature of around -36°C. This confirms that a cooling unit with a cooling capacity of 250 W and a temperature limit of -50°C can be used to reach the target temperature of -30°C. With the acquired knowledge, the implementation of nine temperature system configurations was evaluated on their investment and operating costs, influence of the bearing exchange workflow, space requirements, hazards, flexibility, temperature performance and automation capability. They were rated according to the VDI standard 2225 [65] scoring system and the best system was recommended for the BEAT0.2 test rig. The chosen system is powered by a cooling unit and cooling ducts are placed inside the bearing seat, to provide an efficient heat transfer from the thermal fluid to the bearing. In comparison to the climate chamber solutions, the preferred solution is more flexible, and lower operating costs, a less inconvenient bearing exchange, and a shorter cooling time are expected. The other cooling unit solutions are expected to be more inconvenient when changing bearings. The disadvantage of the preferred system is the necessity of a new housing. In general, automatic hydraulic load application is required in order to utilize the automation capability of the temperature systems. For this temperature system an insulation was designed with the morphological box method. The final design reduces cold losses by a Plexiglas plate between aluminum plate and housing, and also by XPS blocks which are adapted to the housing. The design limits icing by isolating the test rig inside a box. The box can be lifted manually to

gain access to the test rig and is equipped with a seal on the bottom edge. Finally, a thermal model was created in Simulink to determine the specifications for the cooling capacity and supply temperature for future cooling projects. The model was validated with experimental data, resulting in a temperature prediction accuracy with a root mean square error of 1.31 K, but the missing implementation of condensation and solidification heat probably led to cooling time differences. Also more experimental data is needed to evaluate the reliability of the model.

9 Outlook

The evaluation of the temperature systems, the recommendation by the author, and the insulation design give the institute an useful concept for the acquirement of a temperature system for the BEAT0.2 test rig. The detailed engineering of the housing and especially the calculation of the required cooling duct width and the resulting pressure loss will show, if the concept must be adjusted. The thermal model can be further developed with the implementation of the insulation concept, temperature depending material properties, heat generation of the bearing, and condensation and icing processes, but also by comparing the structure of the model to methods in approved literature. With the realization of a cooling system, the thermal model can be further validated with additional temperature measurements at different locations. With continued accurate predictions, the thermal model can be used as a method to determine cooling unit specifications for future cooling projects. In addition, parameter studies can be carried out to optimize the cooling time by changing the supply temperature and cooling capacity.

Bibliography

- [1] Basim Abu-Jdayil et al. "Traditional, state-of-the-art and renewable thermal building insulation materials: An overview". In: *Construction and Building Materials* 214 (2019), pp. 709–735. ISSN: 09500618. DOI: 10.1016/j.conbuildmat.2019.04.102.
- [2] Arne Bartschat, Karsten Behnke, and Matthias Stammler. "The effect of site-specific wind conditions and individual pitch control on wear of blade bearings". In: *Wind Energy Science* 8.10 (2023), pp. 1495–1510. DOI: 10.5194/wes-8-1495-2023.
- [3] Karolina Behrens. BFSV Verpackungsinstitut, Personal correspondence. 26.08.2024.
- [4] Drs. E. Richard Booser and Michael M. Khonsari. "Grease life in ball bearings: The effect of temperatures". In: *Tribology and lubrication technology* (Oct. 2010). https://www.stle.org/images/pdf/stle_org/bok/om_oa/lubrication_fundamentals/grease%20life%20in%20ball%20bearings_the%20effect%20of%20temperatures_tlt%20article_oct10.pdf.
- [5] Ana Briga-Sá et al. "Textile waste as an alternative thermal insulation building material solution". In: *Construction and Building Materials* 38 (2013), pp. 155–160. ISSN: 09500618. DOI: 10.1016/j.conbuildmat.2012.08.037.
- [6] chemie.de. Luftdichte. https://www.chemie.de/lexikon/Luftdichte. html, last accessed: 22.09.2024.
- [7] CiK-Solutions. Klimakammern & Klimaschränke für die hochpräzise Simulation von Temperatur und Feuchte. https://www.cik-solutions.com/pruefkammern-zur-umweltsimulation/klimakammern/, last accessed: 23.09.2024.
- [8] electricity-mangetism.org. Peltier-Effekt Formel | Erklärung & Anwendung. https://www.electricity-magnetism.org/de/peltier-effekt-formel-erklaerung-anwendung/, last accessed: 23.09.2024.
- [9] GESTIS-Stoffdatenbank. GESTIS-Stoffdatenbank. https://gestis.dguv.de/, last accessed: 23.09.2024.
- [10] Rolf Gloor. Kältemaschinen. http://energie.ch/kaeltemaschinen/, last accessed: 22.09.2024. 2020.

- [11] Condair GmbH. h,x Diagramm für feuchte Luft. https://www.condair.de/m/0/hx-diagramm-2017-condair.pdf, last accessed: 23.09.2024.
- [12] MTC Micro Tech Components GmbH. *Thermally conductive paste*. https://www.mtc.de/en/tcp-products/thermally-conductive-paste, last accessed: 23.09.2024.
- [13] SKF Gmbh. Arrangements and their bearing types. https://www.skf.com/il/products/rolling-bearings/principles-of-rolling-bearing-selection/bearing-selection-process/bearing-type-and-arrangement/arrangements-and-their-bearing-types, last accessed: 23.09.2024.
- [14] Douglas Godfrey. "Fretting corrosion or false brinelling?" In: *Tribology and lubrication technology* (Dec. 2003). https://www.stle.org/images/pdf/stle_org/bok/ls/bearings/fretting%20corrosion%20or%20false% 20brinelling_tlt%20article_dec03.pdf.
- [15] Wind energy generation systems Part 1: Design requirements. IEC 61400-1:2019.
- [16] The MathWorks Inc. MATLAB. https://de.mathworks.com/products/matlab.html, last accessed: 23.09.2024.
- [17] Institut für Maschinenkonstruktion und Tribologie. Dauerschwenkprüfstand. https://www.imkt.uni-hannover.de/fileadmin/imkt/Medien/Bilder_Ausstattung/220404_Uebersicht_versuchseinrichtungen-IMKT_kennw.pdf, last accessed: 23.09.2024.
- [18] Bjørn Petter Jelle. "Traditional, state-of-the-art and future thermal building insulation materials and solutions Properties, requirements and possibilities". In: *Energy and Buildings* 43.10 (2011), pp. 2549–2563. ISSN: 03787788. DOI: 10.1016/j.enbuild. 2011.05.015.
- [19] Simen Edsjø Kalnæs and Bjørn Petter Jelle. "Vacuum insulation panel products: A state-of-the-art review and future research pathways". In: *Applied Energy* 116 (2014), pp. 355–375. ISSN: 03062619. DOI: 10.1016/j.apenergy.2013.11.032.
- [20] M. Stammler; O. Menck; Y. Guo; J. Keller. *Wind Turbine Design Guideline DG03: Yaw and Pitch Bearings.* National Renewable Energy Laboratory. 2024.
- [21] HALA Contec GmbH Co. KG. *Datenblätter*. https://www.hala-tec.de/downloads/datenblaetter/, last accessed: 23.09.2024.

- [22] HALA Contec GmbH Co. KG. GAP-FILLER PADS. https://www.hala-tec.de/produkte/gap-filler/, last accessed: 23.09.2024.
- [23] LAUDA DR. R. WOBSER GMBH CO. KG. Integral IN 2560 XTW. https://www.lauda.de/de/produkte/temperiergeraete/thermostate/umwaelz-prozessthermostate/integral-xt-new-generation/details/L002681, last accessed: 23.09.2024.
- [24] Memmert GmbH + Co. KG. Memmert Advanced Peltier App. https://www.memmert.com/de/produkte/klimaschraenke/konstantklima-kammer/, last accessed: 23.09.2024.
- [25] Charles Kolstad. *Lubricant Types, Uses, and Functions.* https://tameson.com/pages/lubricants, last accessed: 23.09.2024. 2021.
- [26] Michael Kuehnel, Falko Hilbrunner, and Thomas Froehlich. *Climate chamber for a high temperature stability*. Tech. rep. Institute of Process Measurement and Sensor Technology, 2011.
- [27] Román de La Presilla et al. "Oscillating rolling element bearings: A review of tribotesting and analysis approaches". In: *Tribology International* 188 (2023), p. 108805. ISSN: 0301679X. DOI: 10.1016/j.triboint.2023.108805.
- [28] leifphysik.de. Änderung der inneren Energie. https://www.leifiphysik.de/waermelehre/innere-energie-waermekapazitaet/grundwissen/aenderung-der-inneren-energie, last accessed: 22.09.2024.
- [29] leifphysik.de. Erster Hauptsatz der Wärmelehre. https://www.leifiphysik.de/waermelehre/innere-energie-waermekapazitaet/grundwissen/erster-hauptsatz-der-waermelehre, last accessed: 22.09.2024.
- [30] Armacell Limited. ArmaFlex Class 0 Technical Data. https://local.armacell.com/fileadmin/cms/singapore/products/en/ArmaflexClass0/ArmaFlex_Class_0_Technical_Guide-web.pdf,lastaccessed: 22.09.2024. 2018.
- [31] Kompetenzzentrum Tribologie Mannheim. Oscillating Rolling Wear Test Bench (SNR-FEB2). https://tribologie-mannheim.de/en/equipment/false-brinelling-test-bench-snr-feb2/, last accessed: 23.09.2024.
- [32] Kok S. Ong, Liben Jiang, and Koon C. Lai. "4.20 Thermoelectric Energy Conversion". In: *Comprehensive Energy Systems.* Elsevier, 2018, pp. 794–815. ISBN: 9780128149256. DOI: 10.1016/B978-0-12-809597-3.00433-8.

- Daniel Overbey. The vapor-compression refrigeration cycle. https://www.buildingenclosure-online.com/blogs/14-the-be-blog/post/90307-vapor-compression-refrigeration-cycle, last accessed: 22.09.2024. 2021.
- [34] A. M. Papadopoulos. "State of the art in thermal insulation materials and aims for future developments". In: *Energy and Buildings* 37.1 (2005), pp. 77–86. ISSN: 03787788. DOI: 10.1016/j.enbuild.2004.05.006.
- [35] peltierpireiri.blogspot.com. *Peltier Element*. https://peltierpireiri.blogspot.com/2017/01/, last accessed: 23.09.2024.
- [36] W Popko et al. *IWES Wind Turbine IWT-7.5-164*. 2018. DOI: 10.24406/IWES-N-518562.
- [37] Yaroslav Porfiryev et al. "Effect of Base Oil Nature on the Operational Properties of Low-Temperature Greases". In: *ACS omega* 5.21 (2020), pp. 11946–11954. DOI: 10.1021/acsomega.9b04087.
- [38] Zwick Roell. Klimakammern für die Materialprüfung. https://www.zwickroell.com/de/zubehoer/klimakammern/#c117489/, last accessed: 23.09.2024.
- [39] Prof. Dr.-Ing. Achim Schmidt. "Wärme- und Stoffübertragung". HAW Hochschule für angewandte Wissenschaften Hamburg. 2020.
- [40] Patrick Schneider and Fatos Xhafa. "Chapter 3 Anomaly detection: Concepts and methods". In: *Anomaly Detection and Complex Event Processing over IoT Data Streams*. Ed. by Patrick Schneider and Fatos Xhafa. Academic Press, 2022, pp. 49–66. ISBN: 978-0-12-823818-9. DOI: https://doi.org/10.1016/B978-0-12-823818-9.00013-4.
- [41] Fabian Schwack et al. "A study of grease lubricants under wind turbine pitch bearing conditions". In: *Wear* 454-455 (2020), p. 203335. ISSN: 00431648. DOI: 10.1016/j. wear. 2020. 203335.
- [42] Fabian Schwack et al. "Time-dependent analyses of wear in oscillating bearing applications". In: *Proceedings of the STLE/ASME International Joint Tribology Conference*. 2017.
- [43] Anton Schweizer. Wärmekapazität Gase. https://www.schweizer-fn.de/stoff/wkapazitaet/wkapazitaet_gase.php, last accessed: 22.09.2024.
- [44] Anton Schweizer. Wärmekapazität verschiedener Materialien. https://www.schweizer-fn.de/stoff/wkapazitaet/wkapazitaet_baustoff_erde.php, last accessed: 22.09.2024.

- [45] Anton Schweizer. Wärmeleitfähigkeit verschiedenen Baumaterialien. https://www.schweizer-fn.de/stoff/wleit_isolierung/wleit_isolierung.php, last accessed: 22.09.2024.
- [46] Anton Schweizer. Wärmeleitfähigkeit verschiedener Metalle. https://www.schweizer-fn.de/stoff/wleit_metall/wleit_metall.php, last accessed: 22.09.2024.
- [47] Anton Schweizer. Wärmeleitfähigkeit verschiedener Metalle. https://www.schweizer-fn.de/stoff/wleit_metall/wleit_metall.php, last accessed: 22.09.2024.
- [48] Anton Schweizer. Wärmeleitfähigkeit von Gase in Abhängigkeit der Temperatur. https://www.schweizer-fn.de/stoff/wleit_gase/wleit_gase.php, last accessed: 22.09.2024.
- [49] Peter Huber Kältemaschinenbau SE. Thermofluide. https://www.huber-online.com/fileadmin/user_upload/huber-online.com/download_center/Broschueren/Huber_Thermofluids_DE-EN.pdf, last accessed: 22.09.2024.
- [50] Peter Huber Kältemaschinenbau SE. *Unistat 1015w*. https://www.huber-online.com/produkte/dynamische-temperiersysteme/unistate-bis-120c/unistat-1015w#wco-productdata-techicaldata, last accessed: 23.09.2024.
- [51] Peter Huber Kältemaschinenbau SE. *Unistat manual*. https://www.huber-online.com/fileadmin/user_upload/huber-online.com/download_center/Betriebsanleitungen/BAL_Unistat_Standard_EN.pdf, last accessed: 23.09.2024.
- [52] Walter Sonderegger and Peter Niemz. "Thermal conductivity and water vapour transmission properties of wood-based materials". In: *European Journal of Wood and Wood Products*, 67 (3) ISSN:0018-3768 ISSN:1436-736X (2009). DOI: 10.3929/ethz-b-000021316.
- [53] Prof. Z. S. Spakovszky. "Thermodynamics and Propulsion". MIT Massachusetts Institute of Technology. 2008.
- [54] H. A. Spikes. "A Thermodynamic Approach to Viscosity". In: *Tribology Transactions* 33.1 (1990), pp. 140–148. ISSN: 1040-2004. DOI: 10.1080/10402009008981940.

- [55] Matthias Stammler. "Endurance Test Strategies for Pitch Bearings of Wind Turbines". PhD thesis. Gottfried Wilhelm Leibniz Universität Hannover, 2020.
- [56] Matthias Stammler. "Low temperature tests at BEAT0.2". Fraunhofer IWES Institute for Wind Energy Systems. 2024.
- [57] Matthias Stammler et al. "Effect of load reduction mechanisms on loads and blade bearing movements of wind turbines". In: *Wind Energy* 23.2 (2020), pp. 274–290. ISSN: 1095-4244. DOI: 10.1002/we.2428.
- [58] Angelantoni Test Technologies. *Praktische Anleitung zur Auswahl einer Klimaprüfkammer*. https://www.acstestchambers.com/de/academy/praktische-anleitung-klimaprufkammer/, last accessed: 23.09.2024.
- [59] thermal-engineering.org. What is Insulation Material Types of Insulation Definition. https://www.thermal-engineering.org/what-is-insulation-material-types-of-insulation-definition/,last accessed: 23.09.2024.
- [60] thermal-engineering.org. What is Thermal Resistance Thermal Resistivity Definition. https://www.thermal-engineering.org/what-is-thermal-resistance-thermal-resistivity-definition/,lastaccessed: 23.09.2024.
- [61] thermal.ferrotec.com. Multi-stage Peltier Thermoelectric Cooler Modules for Large Temperature Differentials. https://thermal.ferrotec.com/products/peltier-thermoelectric-cooler-modules/deep-cooling/, last accessed: 23.09.2024.
- [62] Marko Tošić, Radoslav Tomović, and Janko Jovanovic. "Static Analysis of Internal Load Distribution of the Single Row Deep Groove Ball Bearing". In: Proceedings of the 3rd International Conference Mechanical Engineering in XXI Century, Niš, Serbia (pp. 19-20). Sept. 2015.
- [63] T. M. Tritt. "Thermoelectric Materials: Principles, Structure, Properties, and Applications". In: *Encyclopedia of Materials: Science and Technology.* Elsevier, 2002, pp. 1–11. ISBN: 9780080431529. DOI: 10.1016/B0-08-043152-6/01822-2.
- [64] VDI 2055 Blatt 1 (2008-09-00) Wärme- und Kälteschutz von betriebstechnsichen Anlagen Berechnungsgrundlagen. VDI The Association of German Engineers. 2008.
- [65] *VDI 2225 Blatt 3 (1998-11-00) Technisch-wirtschaftliches Konstruieren*. VDI The Association of German Engineers. 1998.

- [66] Willy Villasmil, Ludger J. Fischer, and Jörg Worlitschek. "A review and evaluation of thermal insulation materials and methods for thermal energy storage systems". In: Renewable and Sustainable Energy Reviews 103 (2019), pp. 71–84. ISSN: 13640321. DOI: 10.1016/j.rser.2018.12.040.
- [67] Alan Wheatley. Shell Global. Personal correspondence. 11.09.2024.